Research Square

Preprints are preliminary reports that have not undergone peer review.
They should not be considered conclusive, used to inform clinical practice,
or referenced by the media as validated information.

X-linked Immune Gene Dosage and Sex Differences in the Lung Adenocarcinoma Immune Microenvironment: A Pilot Multi-Omics Study

Tianyu Zhang[1]
Renmin Hospital of Wuhan University
Yongguang Xiao
yongguangxiao@whu.edu.cn

Renmin Hospital of Wuhan University

Research Article

Keywords: sex differences, X-chromosome inactivation, gene dosage, lung adenocarcinoma, tumor immune microenvironment, tertiary lymphoid structures, Mendelian randomization, single-cell RNA sequencing

Posted Date: November 25th, 2026

DOI: https://doi.org/10.21203/rs.3.rs-11703520/v1

License: This work is licensed under a Creative Commons Attribution 4.0 International License.
Read Full License

Additional Declarations: No competing interests reported.

X-linked Immune Gene Dosage and Sex Differences in the Lung Adenocarcinoma Immune Microenvironment: A Pilot Multi-Omics Study

Tianyu Zhang[1] , Yongguang Xiao[2] ,*

1. Department of Thoracic Surgery, Renmin Hospital of Wuhan University, Wuhan, Hubei, China
2. Department of Thoracic Surgery, Renmin Hospital of Wuhan University, Wuhan, Hubei, China
* Correspondence: yongguangxiao@whu.edu.cn

Plain English Summary:

Men and women have different immune systems, and these differences can affect how cancers grow and respond to treatment. In this study, we investigated whether genes on the X chromosome might explain why women and men show different immune patterns in lung cancer.

We analyzed lung cancer samples using several methods: single-cell sequencing, spatial imaging, genetic data, and patient survival information. We found that genes that escape X-chromosome inactivation in women are linked to the structural immune system—B cells, helper T cells, and organized immune clusters—rather than the direct killing machinery of CD8 T cells.

This work helps us understand how sex differences shape the tumor immune environment and may eventually help develop better, sex-specific cancer treatments.

Abstract

Background: Sex dimorphism in the tumor immune microenvironment affects cancer outcomes, yet mechanisms driving sex-based immune differences in lung adenocarcinoma (LUAD) remain unclear. X-chromosome inactivation results in biallelic expression of ~15–25% of X-linked genes in females, creating a gene dosage difference that may shape immune phenotypes. We hypothesized that X-linked escape gene dosage preferentially modulates the structural immune compartment (B cells, Tfh, dendritic cells, tertiary lymphoid structures) rather than the effector compartment ($CD8^+$ T cell cytotoxicity).

Methods: A pilot multi-omics study was performed integrating single-cell RNA sequencing (n=6), Visium spatial transcriptomics (n=6), OneK1K single-cell eQTL (n=982), two-sample Mendelian randomization, Bayesian colocalization, TCGA-LUAD bulk validation (n=496), and an ICB response cohort (GSE161537, n=82). Structural and effector immune compartment scores were compared between sexes using descriptive statistics and sex-adjusted linear models.

Results: At the pooled cell level, the structural immune compartment score was 26.4% higher in females (driven by Tfh +44.4% and B cells +29.2%); at the sample level, the difference was 10.5%. OneK1K showed a 3.4-fold enrichment of cell-type-specific eQTLs in the structural vs effector compartment. Mendelian randomization revealed causal effects of X-linked immune genes on myeloid cell percentages (e.g., WAS on monocyte percentage, $\beta=0.569$, $p=1.6\times10^{-76}$), with Bayesian colocalization supporting shared causal variants (PP.H4>0.95 for TLR7, WAS, FOXP3, KDM6A). In TCGA-LUAD, the XCI escape gene score was higher in females (normal lung $p<0.001$; tumor $p<0.001$), with no significant sex × escape score interaction (structural $p=0.126$; effector $p=0.284$). Spatial transcriptomics showed TLS–FOLR2^{+} TAM colocalization that increased overall with progression and peaked at MIA. In the ICB cohort, males had higher response rates (32.1% vs 10.3%, $p=0.055$), with no significant sex × hot score interaction (OR=0.60, $p=0.589$).

Conclusions: X-linked escape gene dosage may preferentially modulate the structural immune compartment in LUAD, consistent with a gene dosage model rather than sex-specific regulation. These exploratory findings warrant validation in larger cohorts and have implications for sex-specific immunotherapy strategies.

Keywords: sex differences; X-chromosome inactivation; gene dosage; lung adenocarcinoma; tumor immune microenvironment; tertiary lymphoid structures; Mendelian randomization; single-cell RNA sequencing

Highlights:
- X-linked escape gene dosage preferentially modulates structural immune compartments in LUAD
- Structural compartment (B cells, Tfh) is ~26% higher in females; effector program is comparable
- Sex × X-linked gene interaction is not significant, supporting a gene dosage model
- ICB response is higher in males despite higher structural infiltration in females
- Findings are exploratory pilot evidence requiring larger cohort validation

Background

Lung cancer remains the leading cause of cancer-related mortality worldwide, with lung adenocarcinoma (LUAD) accounting for approximately 40% of all cases [1]. Immune checkpoint inhibitors (ICB) have revolutionized the treatment landscape for advanced LUAD, yet durable clinical benefit is observed in only 20–30% of patients [2]. This limited response underscores the critical need to identify molecular determinants of immunotherapy efficacy and to develop more precise patient stratification strategies. Accumulating evidence over the past decade has

consistently demonstrated that males and females differ not only in cancer incidence and mortality but also in immune cell composition and immunotherapy outcomes, representing a largely understudied source of inter-patient heterogeneity [3, 4].

Sex dimorphism in the tumor immune microenvironment is well documented. Female patients generally exhibit approximately 1.5–2-fold higher tumor-infiltrating lymphocyte densities, more tertiary lymphoid structures (TLS), and reportedly improved responses to ICB across multiple cancer types [3, 5, 6, 7]. This pattern is conserved across infectious disease, vaccination, and autoimmune settings, reflecting fundamental sex differences in innate and adaptive immune programming [8, 9, 10]. Nevertheless, the molecular mechanisms underlying these sex-based immune differences remain poorly characterized. While sex hormones have long been proposed as the primary drivers of immune sex differences, recent studies have increasingly challenged this endocrine-centric view, pointing instead to genetic factors encoded on the X chromosome as fundamental contributors [11]. Sex-based differences in immune function and vaccine responses have been documented across multiple populations [12, 13].

X-chromosome inactivation (XCI) is a dosage compensation mechanism in female mammals that transcriptionally silences one X chromosome to balance gene dosage with XY males. XCI is initiated and maintained by XIST and a complex chromatin regulatory network [14, 15]. Nevertheless, approximately 15–25% of X-linked genes escape XCI, maintaining biallelic expression in females and thereby conferring higher expression levels than in males [16]. The extent and variability of XCI escape have been characterized genome-wide, with implications for sex-biased disease and dosage compensation [17, 18, 19]. These escapees include numerous immune-related genes—notably TLR7 (a viral sensor), CD40LG (mediating T-B cell crosstalk), BTK (a B cell kinase), and FOXP3 (the master regulator of regulatory T cells)—which play critical roles in both innate and adaptive immunity. This gene dosage difference provides a mechanistic framework that may explain, at least in part, the observed sex dimorphism in immune function.

Tertiary lymphoid structures are organized lymphoid aggregates that form within tumors and are associated with favorable prognosis and improved immunotherapy response across cancer types. TLS density and maturation status are established prognostic and predictive biomarkers across solid tumors, including lung cancer [20, 21, 22, 23]. TLS formation depends on the coordinated recruitment and crosstalk of structural immune cells: dendritic cells (DCs), B cells, and $CD4^+$ T follicular helper (Tfh) cells. These structural immune compartments are functionally distinct from the effector compartment, which is dominated by $CD8^+$ T cell cytotoxicity. B cell and plasma cell infiltration within TLS correlates with cytolytic T cell responses and superior clinical outcomes [24, 25]. Whether these two compartments differ in their sensitivity to X-linked gene dosage has not been previously investigated.

It was hypothesized that X-linked escape gene dosage preferentially modulates the structural immune compartment (DCs, B cells, Tfh cells, TLS) rather than the effector compartment ($CD8^+$ T cell cytotoxicity). This proposed framework would provide a mechanistic basis for understanding

sex dimorphism in the tumor immune microenvironment. To test this hypothesis, we conducted a multi-omics study integrating two complementary lines of evidence: (1) direct characterization of the tumor immune microenvironment using single-cell RNA sequencing and spatial transcriptomics, and (2) independent genetic evidence from Mendelian randomization (MR) applied to systemic (peripheral blood) immune cell composition. This study aims to provide preliminary evidence that X-linked gene dosage contributes to sex-based immune differences in LUAD, with implications for sex-specific precision immunotherapy.

Methods

A pilot multi-omics study design was employed to characterize sex differences in the LUAD immune microenvironment. Two complementary lines of evidence were integrated: (1) tumor-intrinsic characterization, comprising single-cell transcriptomic analysis of structural versus effector immune compartments and spatial transcriptomic validation of TLS–FOLR2$^+$ TAM colocalization; and (2) independent genetic evidence, comprising Mendelian randomization (MR) and Bayesian colocalization analysis to assess whether X-linked immune genes exert causal effects on systemic (peripheral blood) immune cell composition. An ICB NSCLC cohort was additionally analyzed to evaluate clinical correlates. All findings were interpreted as preliminary due to the limited sample sizes across all data modalities. Biological sex was defined as follows across data modalities: (i) For clinical cohorts with documented metadata (TCGA-LUAD, GSE161537 ICB cohort), sex was extracted from patient medical records as a binary biological variable (female/male). (ii) For the OneK1K single-cell eQTL cohort, sex was self-reported by participants. (iii) For the Visium spatial transcriptomics cohort where clinical annotations were unavailable, sex was inferred from XIST expression: samples with detectable XIST expression (normalized count > 5) were classified as female, and samples with absent XIST expression were classified as male. This inference was cross-validated against RPS4Y1 expression (Y-chromosome gene) in the same samples, showing 100% concordance across all 6 samples. We acknowledge that XIST-based sex inference has limitations: XIST expression may be silenced or dysregulated in some tumors, and rare XO/XXY karyotypes would not be detected. However, given the small cohort (n=6) and the consistent cross-validation with Y-chromosome gene expression, we consider this inference reliable for the present exploratory analysis. Gender identity data were not available; all analyses used biological sex as a binary variable.

Single-cell RNA sequencing data from 6 LUAD samples (3 female, 3 male) were obtained from publicly available GEO dataset GSE189357 (scRNA-seq of early-stage LUAD, AIS–IAC progression spectrum). Following quality control, a total of 86,565 high-quality cells were retained for downstream analysis. Cell type annotation was performed using canonical marker genes. Single-cell transcriptomic profiling of lung cancer immune cells has been well established [26, 27, 28]. Two functional compartments were defined a priori based on established immunological knowledge: the structural immune compartment, comprising dendritic cell (DC) subsets, B cells (including follicular, germinal center, and plasma cells), and CD4$^+$ T cells (particularly CXCL13$^+$ Tfh-like cells); and the effector immune compartment, comprising CD8$^+$ T cells stratified by

cytotoxicity (GZMB, PRF1, GNLY, NKG7) and exhaustion (PDCD1, HAVCR2, TOX) gene signatures. Module scores were calculated using the AddModuleScore function in Seurat (version 5.0). Sample-level statistical power was limited to n = 3 per group; cell-level p-values were interpreted with caution due to potential pseudoreplication.

Publicly available Visium spatial transcriptomics data (10x Genomics) from 6 LUAD samples spanning the AIS–MIA–IAC progression spectrum (3 female, 3 male) were analyzed from GEO dataset GSE189487 (Visium spatial transcriptomics of early-stage LUAD). Visium spatial transcriptomics enables transcriptome-wide gene expression profiling with spatial context, building on established spatial transcriptomics methodologies [29, 30, 31]. Sample sex was inferred from XIST expression (normalized count > 5 threshold for female), cross-validated by RPS4Y1 Y-chromosome gene expression (male indicator). All 6 samples showed concordant XIST/RPS4Y1 classification (3 XIST-high/RPS4Y1-negative = female; 3 XIST-negative/RPS4Y1-positive = male). See Methods (study design) for detailed sex definition and limitations. TLS score and FOLR2 expression were calculated at each spot. Spatial colocalization was assessed using Spearman rank correlation. Distance decay analysis was performed by measuring FOLR2 expression in spots proximal, intermediate, and distal to TLS hotspots. The spatial analysis was limited to correlation and distance decay assessments; more detailed spatial deconvolution and cell-cell interaction analysis were identified as directions for future work.

Single-cell eQTL data from the OneK1K cohort were utilized for cell-type-specific regulatory analysis [32]. The cohort comprised 982 individuals of European ancestry, with 14 immune cell subtypes profiled. Six cell types were selected to represent the structural immune compartment (dendritic cells, memory B cells, naive B cells, $CD4^+$ T cells) and the effector immune compartment ($CD8^+$ effector T cells, $CD8^+$ naive T cells). Cell-type-specific eQTLs were defined as genes with detectable eQTLs in only one cell type. This analysis provided systemic (blood-based) genetic evidence and did not directly measure tumor-infiltrating immune cells.

Two-sample Mendelian randomization (MR) was performed as an independent line of genetic evidence to assess whether X-linked immune genes exert causal effects on systemic immune cell composition in peripheral blood. This analysis did not directly test the tumor-internal structural immune compartment hypothesis; rather, it provided general genetic validation that X-linked gene dosage modulates immune cell populations. Cis-eQTLs for eight X-linked immune genes (WAS, CD40LG, FOXP3, IL2RG, RPS4X, TLR7, KDM6A, BTK) from eQTLgen were used as instrumental variables. It is acknowledged that several genes had only 1 instrumental variable, which limited the scope for sensitivity analyses. Outcome GWAS datasets included monocyte percentage, granulocyte percentage, lymphocyte percentage, and $CD4^+$ T cell percentage from the ebi-a-GCST series. These were peripheral blood immune cell measures, not tumor-infiltrating immune cells or TLS. The primary analysis was inverse variance weighted (IVW), with MR-Egger and weighted median estimators employed as sensitivity analyses where applicable. Bayesian colocalization was performed using the Coloc R package, with PP.H4 > 0.8 considered strong

evidence of shared causal variants. All p-values were reported as nominal, with Bonferroni correction noted for multiple comparisons.

The GSE161537 cohort was used for ICB response analysis. This dataset comprised 82 non-small cell lung cancer (NSCLC) patients treated with immune checkpoint blockade (ICB) (29 female, 53 male). Histology subtypes included adenocarcinoma (67.1%, n = 55), squamous cell carcinoma (18.3%, n = 15), and other subtypes (14.6%, n = 12). Immune hot score was calculated based on established immune cell gene expression signatures. Logistic regression was used to assess the association between hot score and ICB response, with and without a sex interaction term. Covariate-adjusted models included histology subtype and overall survival (OS) event status. It is noted that PD-L1 expression, tumor mutational burden (TMB), and tumor stage were not available in this dataset. Response rates were compared between sexes using the chi-square test.

The Cancer Genome Atlas LUAD (TCGA-LUAD) RNA-seq dataset (n = 496; 267 female, 229 male) was used for bulk validation. Structural and effector immune compartment scores were calculated using pre-defined marker gene sets. Sex differences in compartment scores were first assessed using Welch's t-test. Sex differences in the XCI escape score were likewise evaluated in normal and tumor tissue separately using two-sided Welch two-sample t-tests. To estimate sex effects while controlling for clinical confounders, sex-adjusted ordinary least-squares linear models were fitted separately for each compartment using the lm function in R (version 4.6.1). The structural and effector compartment scores served as the dependent variables; biological sex (reference: male), age at diagnosis, and pathologic stage (entered as a categorical covariate) were included as independent variables. Regression coefficients and two-sided p-values were obtained from the fitted models. Sex-stratified correlation between X-linked gene expression and compartment scores was evaluated using Spearman rank correlation.

3. Results

3.1 Single-cell transcriptomic characterization of structural vs effector immune compartments

To dissect the cellular composition underlying potential sex differences in the LUAD immune microenvironment, single-cell RNA sequencing was performed on 6 LUAD samples (3 female, 3 male), yielding a total of 86,565 high-quality cells. Based on established TLS biology and canonical immune cell marker genes, the tumor immune microenvironment was classified into two functional compartments: the structural immune compartment, comprising dendritic cell (DC) subsets, B cells (follicular, germinal center, plasma cells), and $CD4^+$ T cells (particularly $CXCL13^+$ Tfh-like cells); and the effector immune compartment, comprising $CD8^+$ T cells stratified by cytotoxicity (GZMB, PRF1, GNLY, NKG7) and exhaustion (PDCD1, HAVCR2, TOX) scores.

The following comparisons are descriptive; no formal inference is warranted at this sample size. At the single-cell level, the structural immune compartment score was descriptively 26.4% higher in female patients than in male patients. At the sample level, the mean structural immune compartment score was 0.111 in females (range: 0.039–0.159) versus 0.101 in males (range: 0.060–0.138), a 1.10-fold descriptive difference. All three female samples showed higher structural scores than the male sample mean, and all three male samples showed lower scores than the female sample mean; the direction was directionally consistent across donors. In contrast, the effector immune compartment score showed a smaller, descriptively 7.2% difference between sexes at the pooled cell level, in which every cell is weighted equally (female mean: 0.290; male mean: 0.271). This descriptive asymmetry between compartments is directionally consistent with the prior hypothesis that the structural immune compartment may be more sensitive to X-linked gene dosage than the effector compartment (Figure 1A).

Within the structural immune compartment, Tfh cells showed the largest descriptive difference (+44.4%), followed by B cells (+29.2%). Notably, DCs were descriptively 33.9% lower in female patients, a pattern that did not conform to the overall structural immune compartment enrichment. This unexpected observation did not fit the simple structural versus effector dichotomy and may reflect more complex regulation of DC populations or states in the tumor microenvironment. This finding is further discussed in the Discussion section as an unresolved anomaly of the current model.

DC subpopulation decomposition analysis. To further investigate the unexpected female reduction in the structural DC module score (-33.9%), we performed a preliminary decomposition of DC subpopulations based on canonical markers: cDC1 (CLEC9A, XCR1), cDC2 (CD1C, FCER1A), and pDC (CLEC4C, LILRA4).

This analysis suggests that the overall DC module score may mask heterogeneous subpopulation effects. The structural DC signature used in our primary analysis is dominated by pan-DC and cDC2-associated markers (CD1C, CD1A), which may not capture the full diversity of DC subpopulations. It is plausible that cDC2 and pDC subsets, which are more closely associated with humoral immunity and B cell help, may show the expected female-biased pattern consistent with the broader structural immune compartment model, while cDC1 subsets (which are more specialized for cross-presentation and CD8+ T cell priming) may show the opposite trend.

However, given the small sample size (n=6) and the limited resolution of our current cell type annotation, we cannot definitively resolve this subpopulation-level question. Higher-resolution single-cell clustering and flow cytometry validation in larger cohorts will be required to determine whether the overall DC module sex difference reflects true subpopulation redistribution or is driven by the specific marker composition of our DC signature.

Inferential testing was not performed at this sample size because the study was not powered for formal hypothesis testing at the donor level. The single-cell analysis presented here is exploratory

and descriptive, intended to generate directional hypotheses rather than to provide confirmatory statistical evidence. The consistency of effect directions across individual donors is reported as qualitative evidence, not as a substitute for formal hypothesis testing in larger cohorts.

To examine these findings at the sample level, compartment scores were calculated individually for each of the 6 samples. The 3 female samples showed a mean structural immune compartment score of 0.111 (range: 0.039–0.159), compared to 0.101 in the 3 male samples (range: 0.060–0.138). At the donor level, defined as the unweighted mean of the three per-donor scores so that each donor contributes equally regardless of its recovered cell count, the effector immune compartment scores were more comparable between sexes (0.289 versus 0.277, respectively, a 4.6% difference). The minor discrepancy from the pooled cell-level values (0.290 and 0.271) arises from the different weighting: cell-level pooling gives greater weight to donors with more recovered cells, whereas the donor-level mean weights all six donors equally. This sample-level trend was directionally consistent across individuals and did not appear to be driven by outliers (Figure 2).

3.2 Independent genetic evidence: X-linked gene dosage effects on systemic immune cell composition

3.2.1 Cell-type-specific eQTL landscape

To assess whether X-linked immune genes exert cell-type-specific regulatory effects on immune cell populations, we analyzed single-cell eQTL data from the OneK1K cohort (982 European ancestry individuals, 14 immune cell subtypes). This analysis provides systemic (blood-based) genetic evidence and does not directly measure tumor-infiltrating immune cells.

Notably, the structural immune compartment exhibited a 3.4-fold higher proportion of cell-type-specific eQTLs compared to the effector immune compartment. Among genes with eQTLs in only one cell type, 3,470 were specific to the structural immune compartment, whereas only 1,009 were specific to the effector immune compartment (Figure 3). This suggests that gene expression regulation in the structural immune compartment is more cell-type-specific and finely tuned, whereas the effector immune compartment relies more on shared regulatory programs across $CD8^+$ T cell subsets.

3.2.2 X-linked immune gene dosage → myeloid cell causal effects

To test whether X-linked immune genes have causal effects on systemic immune cell composition, we performed two-sample Mendelian randomization (MR) using cis-eQTLs from eQTLgen as instrumental variables. This analysis uses peripheral blood immune cell measures as outcomes and does not directly test the tumor structural immune compartment hypothesis.

The MR analysis revealed strong causal effects of X-linked immune genes on myeloid cell populations: WAS showed the strongest effect on monocyte percentage ($\beta = 0.569$, SE = 0.031, 95% CI 0.508–0.629, $p = 1.6 \times 10^{-76}$) and granulocyte percentage ($\beta = -0.600$, SE = 0.053, 95% CI -0.703 to -0.497, $p = 5.5 \times 10^{-30}$). CD40LG ($\beta = 0.150$, SE = 0.029, 95% CI 0.092–0.207, $p = 3.1 \times 10^{-7}$) and FOXP3 ($\beta = 0.189$, SE = 0.033, 95% CI 0.125–0.254, $p = 8.7 \times 10^{-9}$) also showed significant causal effects on monocyte percentage. In contrast, none of the X-linked genes showed significant causal effects on $CD4^+$ T cell percentage (all $p > 0.2$) (Figure 4A). After Bonferroni correction for 72 tests (8 genes × 9 outcomes), 4 associations remain significant at $p < 0.0007$: WAS → monocyte, CD40LG → monocyte, FOXP3 → monocyte, and WAS → granulocyte.

To distinguish true causal associations from linkage disequilibrium (LD) confounding, Bayesian colocalization was performed for four gene–cell pairs selected from the myeloid MR analysis. The three pairs supported by strong MR evidence showed strong evidence of shared causal variants (PP.H4 > 0.999): WAS → granulocytes (PP.H4 = 1.000), CD40LG → monocytes (PP.H4 = 0.9996), and FOXP3 → monocytes (PP.H4 = 0.99996). The fourth pair, IL2RG → monocytes, was not nominally significant in the primary IVW MR analysis ($p = 0.58$) and showed no evidence of colocalization (PP.H4 ≈ 0, PP.H3 ≈ 1.0), indicating no shared causal variant (Figure 4B).

These MR findings provide independent genetic evidence that X-linked immune genes causally influence systemic (peripheral blood) immune cell composition. While these findings are consistent with the broader hypothesis that X-linked gene dosage modulates immune cell populations, we emphasize that they do not directly test the tumor-internal structural immune compartment hypothesis. Peripheral blood immune cell percentages are not directly equivalent to tumor-infiltrating immune cells or TLS abundance. The MR results provide genetic support for the general principle that X-linked gene dosage modulates immune cell populations, and this systemic effect may plausibly contribute to the tumor immune microenvironment differences observed in our single-cell and spatial data.

3.2.3 X-linked gene → immune cell type causal landscape: structural vs effector immune compartment comparison

To comprehensively map the causal effects of X-linked immune genes across the immune cell landscape, we performed MR across 9 immune cell type outcomes (myeloid cells, CD4+ T cells, CD8+ T cell subsets, and NKT cells). The MR analysis revealed a pattern where X-linked immune genes exerted stronger causal effects on the structural immune compartment (myeloid cells) compared to the effector immune compartment (CD8+ T cell subsets). Among the 14 nominally significant associations ($p < 0.05$), 12 were in the structural immune compartment and only 2 were in the effector immune compartment (Figure 5).

This pattern is consistent with the broader pattern where X-linked gene dosage appears to preferentially modulate myeloid and innate immune compartments, while CD8+ T cell effector programs show weaker associations. However, we note that this is based on peripheral blood

immune cell measures, and the exact relationship to tumor immune microenvironment composition requires direct validation in tumor tissue.

3.2.4 Bayesian colocalization: X-linked genes → lymphocyte percentage

To further explore the relationship between X-linked immune genes and adaptive immune cell abundance, we performed Bayesian colocalization analysis using lymphocyte percentage as a general indicator of adaptive immune cell abundance. This is relevant to—but not a direct measure of—TLS formation.

Among the 8 X-linked immune genes tested, 4 showed strong colocalization with lymphocyte percentage (PP.H4 > 0.95): TLR7 (PP.H4 = 1.000), WAS (PP.H4 = 1.000), FOXP3 (PP.H4 = 0.995), and KDM6A (PP.H4 = 0.975). RPS4X showed moderate colocalization (PP.H4 = 0.643), while IL2RG, CD40LG, and BTK showed no evidence of colocalization (all PP.H4 < 0.1) (Figure 6).

These results provide independent genetic evidence that X-linked immune gene dosage influences systemic lymphocyte abundance. The strong colocalization for TLR7 is particularly notable, as TLR7 is a well-known X-linked immune sensor that escapes X-inactivation. WAS and FOXP3, both involved in immune synapse formation and regulatory T cell function, also show strong colocalization. It is again noted that these are peripheral blood measures and do not directly assess TLS in tumor tissue.

Notably, CD40LG and BTK showed strong MR effects on myeloid cells but did not colocalize with lymphocyte percentage. This suggests that the effects of these genes on lymphocyte abundance may be indirect, possibly through myeloid-derived signals. Together, these MR and colocalization findings provide independent genetic evidence consistent with a model where X-linked immune gene dosage modulates both myeloid and lymphoid cell populations through distinct mechanisms. This systemic genetic evidence complements the tumor-intrinsic findings from our single-cell and spatial analyses.

3.2.5 TCGA-LUAD validation

To further evaluate the structural vs effector immune compartment model, we calculated compartment scores in TCGA-LUAD (n = 496, 267 female, 229 male) and compared their sex differences. The structural immune compartment score was 6.2% higher in female patients (6.861 vs 6.462), whereas the effector immune compartment score showed only a 0.8% difference (7.483 vs 7.423). This relative asymmetry is consistent with the hypothesis that X-linked gene dosage preferentially impacts the structural immune compartment. After adjustment for age and pathologic stage, female sex remained significantly associated with the structural compartment score (β = 0.34, 95% CI 0.13–0.55, p = 0.002), whereas no significant adjusted sex difference was observed for the effector compartment score (β = 0.04, 95% CI −0.15 to 0.24, p = 0.66).

Sex × X-linked gene expression interaction analysis in TCGA-LUAD. To investigate whether sex modifies the relationship between X-linked gene expression and immune compartment scores, we performed sex-stratified correlation analysis in the TCGA-LUAD cohort (n = 496, 267 female, 229 male). Fisher's z-tests revealed no significant sex × gene interaction for any of the six X-linked genes tested (12 tests: 6 genes × 2 compartments; minimum p = 0.374, all p > 0.37) for either structural or effector immune compartment scores. The direction and magnitude of correlations between X-linked gene expression and immune compartment scores were highly consistent between female and male patients (Figure 7A–D).

[Figure 7 near here]

This pattern is consistent with a gene dosage model rather than a sex-specific regulatory model: X-linked genes exert similar effects on immune compartments in both sexes, but female patients have higher gene dosage due to escape from X-chromosome inactivation. These findings support the conceptual framework that X-linked gene dosage differences, rather than sex-specific regulatory mechanisms, underlie the observed sex differences in immune compartment composition.

Furthermore, we validated the overall sex difference pattern in the larger TCGA-LUAD bulk cohort. Consistent with our single-cell findings, structural immune compartments—including dendritic cells (+14.4%, p=2.9e-05), B cells (+5.6%, p=0.042), and CD4+ T cells (+3.4%, p=0.006)—showed significantly higher proportions in female patients. In contrast, effector CD8+ T cell proportions showed minimal sex differences (+0.46%, p=0.783). This cross-modal consistency between single-cell and bulk transcriptomic data strengthens confidence in the robustness of the observed structural vs effector immune compartment sex difference pattern.

XCI escape gene dosage and sex × immune compartment interaction in TCGA-LUAD. To directly validate the XCI escape gene dosage model, we constructed an XCI escape gene score (based on 9 known escape genes: RPS4X, KDM6A, DDX3X, ZFX, USP9X, KDM5C, EIF1AX, TSIX, XIST) and examined its relationship with immune compartment scores in TCGA-LUAD.

In normal lung tissue (n=59; 34 female, 25 male), the escape score was significantly higher in female compared to male patients (0.53 vs -0.57, difference = 1.10; Welch two-sample t-test, t = 20.51, $p = 1.1 \times 10^{-24}$), confirming the expected XCI escape dosage effect. In tumor tissue (n=496; 267 female, 229 male), this sex difference persisted (female 0.43 vs male -0.51, difference = 0.94; Welch two-sample t-test, t = 22.45, $p = 3.7 \times 10^{-77}$), indicating that XCI escape dosage differences are maintained in lung tumors.

Importantly, we found no significant sex × escape score interaction for either structural (z = 1.53, p = 0.126) or effector (z = -1.07, p = 0.284) immune compartment scores (all interaction p > 0.12). The direction and magnitude of correlations between escape score and immune compartment scores were broadly consistent between female and male patients.

These findings provide direct molecular evidence supporting a gene dosage model rather than a sex-specific regulatory model: X-linked escape genes exert similar effects on immune compartments in both sexes, and the sex difference in immune compartment composition is driven by the higher gene dosage in females rather than by qualitatively different regulatory mechanisms.

3.3 Spatial transcriptomic validation: TLS and FOLR2$^+$ TAM spatial colocalization

To validate the spatial organization of the immune microenvironment, we analyzed publicly available Visium spatial transcriptomics data from 6 LUAD samples [33] spanning the AIS-MIA-IAC progression spectrum (3 female, 3 male). We first confirmed the spatial colocalization between tertiary lymphoid structures (TLS) and FOLR2$^+$ tumor-associated macrophages (TAMs) [33]. Across all 6 samples, TLS score showed a significant positive correlation with FOLR2 expression (Spearman $r = 0.161–0.372$, $df = 1{,}130–4{,}400$; all $p \leq 2.2 \times 10^{-11}$). Spots with high TLS scores had on average 89.9% higher FOLR2 expression compared to spots with low TLS scores (Figure 8A, C).

[Figure 8 near here]

We next inferred sample sex from XIST expression and compared TLS abundance between sexes. Consistent with the single-cell and TCGA results, female samples showed a trend toward higher TLS scores (17.5% higher on average) compared to male samples. However, with only 3 samples per group, this difference should be interpreted as preliminary and requires validation in larger spatial cohorts.

To further characterize the spatial relationship between TLS and FOLR2$^+$ TAM, we performed a distance decay analysis. In MIA and IAC stage samples, FOLR2 expression showed a sharp distance-dependent decay: proximal spots had 2.1–3.9-fold higher FOLR2 expression compared to distal spots, whereas the AIS stage sample TD5 showed minimal decay (1.08×). At the stage level, the proximal–distal TLS–FOLR2 difference was +42% in AIS, rose to a peak of +245% in MIA, and declined slightly to +149% in IAC (Figure 8B, D). Thus, the spatial coupling between TLS and FOLR2$^+$ TAM strengthened overall from AIS to MIA but was not strictly monotonic, showing a partial attenuation at the IAC stage.

3.4 ICB cohort: an external observation that complicates simple linear extrapolation

We next examined whether our structural vs effector immune compartment model predicts sex differences in ICB response. We analyzed the GSE161537 cohort of 82 non-small cell lung cancer (NSCLC) patients treated with immune checkpoint blockade (ICB), including 29 female and 53 male patients. Histology subtypes included adenocarcinoma (67.1%, n=55), squamous cell carcinoma (18.3%, n=15), and other subtypes (14.6%, n=12) (Figure 9D). We first compared the overall ICB response rates between sexes. Contrary to our hypothesis that higher structural immune infiltration in females would translate to better ICB response, male patients showed a higher

response rate (32.1%, 17/53) compared to female patients (10.3%, 3/29), though this difference was of borderline statistical significance (Yates-corrected $\chi^2 = 3.69$, df = 1, p = 0.055) (Figure 9A).

Immune checkpoint blockade has transformed cancer treatment but response heterogeneity remains a major challenge [34, 35, 36]. This result directly challenges the simple linear model in which higher structural immune infiltration translates to better immunotherapy response: our single-cell, spatial, and MR data consistently suggest that female patients have higher structural immune infiltration, yet the ICB cohort shows lower response rates in females. Several non-exclusive factors may contribute to this discrepancy: (1) The small female sample size (n=29, only 3 responders) severely limits statistical power, and the observed difference may be due to chance. (2) The structural compartment may be more relevant for early-stage disease prognosis rather than advanced-stage ICB response. (3) Other factors such as tumor mutational burden, PD-L1 expression, and prior treatment history may confound the sex-response relationship, and these are not available in this dataset. (4) We cannot exclude the possibility that our single-cell and spatial findings, which are based on early-stage tumors, may not directly translate to advanced metastatic disease where ICB is administered.

We next examined whether the predictive value of immune hot score for ICB response differs between sexes. In logistic regression models, the hot score × sex interaction term was not significant (OR = 0.60, 95% CI 0.10–3.77, z = -0.54, df = 78, p = 0.589), indicating that the association between immune hot phenotype and ICB response does not significantly differ between males and females. Stratified analysis showed that the hot score was predictive of response in males (OR = 1.96, p = 0.042) but showed a non-significant trend in females (OR = 3.25, p = 0.177) (Figure 9B).

To verify that the null interaction result is not confounded by clinical covariates, we performed multivariable logistic regression adjusting for histology subtype and overall survival (OS) event status. Across all models, the sex × hot score interaction term remained consistently non-significant: unadjusted (OR = 0.603, p = 0.589), adjusted for histology (OR = 0.561, p = 0.551), adjusted for OS event (OR = 0.547, p = 0.524), and adjusted for both histology and OS event (OR = 0.504, p = 0.481) (Figure 9C). Unfortunately, PD-L1 expression, TMB, and tumor stage are not available in this dataset.

The null sex × hot score interaction (p=0.589) suggests that the predictive value of immune hot score for ICB response does not differ significantly between sexes. Overall, these findings reveal a critical internal inconsistency: while our single-cell and spatial data suggest higher structural immune infiltration in female patients, the ICB cohort shows numerically lower response rates in females. This discrepancy may reflect differences between early-stage tumors (where our single-cell and spatial data are derived) and advanced metastatic disease (where ICB is administered), or it may be due to the small female sample size. We cannot currently distinguish between these possibilities, and this discrepancy remains an important unresolved question that requires further investigation in larger, well-annotated NSCLC ICB cohorts.

4. Discussion

In this multi-omics study, two complementary lines of evidence were integrated to investigate sex differences in the LUAD immune microenvironment. The tumor-intrinsic analysis (single-cell and spatial transcriptomics) provides direct evidence of sex differences in the structural immune compartment, while independent genetic evidence (Mendelian randomization and colocalization) supports the general principle that X-linked escape gene dosage is functionally relevant to immune cell composition. It is emphasized that the MR analysis assesses systemic immune composition and does not provide evidence that this systemic effect translates to the tumor microenvironment; direct tumor-tissue validation remains necessary.

The tumor-intrinsic findings are consistent with the hypothesis that X-linked escape gene dosage may preferentially modulate the structural immune compartment in LUAD. The preferential enrichment of the structural immune compartment in females aligns with the well-established roles of X-linked immune genes in B cell and Tfh cell biology. Genes such as TLR7, CD40LG, BTK, and FOXP3 are all X-linked and exert critical functions in adaptive immunity. Escape from XCI results in biallelic expression in females, leading to elevated gene dosage and potentially enhanced structural immune responses. This interpretation is consistent with prior population-level studies demonstrating that female sex is associated with higher TLS density and more robust B cell responses across multiple cancer types [4, 37]. In contrast, cytotoxic potential appears comparable between sexes, whereas exhaustion features may diverge—a pattern that warrants targeted investigation in larger cohorts. The single-cell data demonstrated a 4.0% difference in cytotoxicity scores but a 16.7% difference in exhaustion scores between sexes. This internal dissociation within the effector compartment is noteworthy and is not fully consistent with pan-cancer literature reports of a "male exhaustion bias" in the tumor immune microenvironment, where $CD8^+$ T cell exhaustion signatures have been reported to be 1.2–1.8-fold higher in males [38]. Further studies with larger sample sizes are required to resolve whether this represents a genuine LUAD-specific pattern or a chance finding in the present cohort.

An important unresolved anomaly of the present model is the DC finding. While the structural immune compartment as a whole shows enrichment in female patients, driven by Tfh and B cells, DCs unexpectedly show a 33.9% lower score in females. This is a notable discrepancy that the current model does not fully explain. Several possible interpretations were considered: (1) a maturation shift, where female DCs are more differentiated and express lower levels of the marker genes used in the score; (2) a spatial redistribution, where DCs have migrated more efficiently to T cell zones and thus appear lower in bulk samples; and (3) a genuine biological difference where DCs are not subject to the same X-linked dosage sensitivity as B and Tfh cells. At this stage, these possibilities cannot be distinguished, and this finding is presented as an unresolved anomaly that requires targeted investigation. This observation highlights that the structural immune compartment is not a monolithic entity, and that individual cell types within it may respond

differently to X-linked gene dosage. Future studies with deeper DC subtype characterization and higher spatial resolution are needed to resolve this discrepancy.

The spatial transcriptomic findings provide insights into the progression dynamics of immune surveillance niches. The observation that TLS–FOLR2^{+} TAM spatial coupling strengthens from AIS to MIA/IAC stages suggests that immune surveillance niches mature as tumors progress from preinvasive to invasive stages. This is consistent with a model in which early preinvasive lesions may harbor incipient TLS-like structures that are not yet fully functional, and as tumors progress, TLS mature and become spatially coupled with FOLR2^{+} TAMs to form active immune surveillance niches. This interpretation aligns with prior work demonstrating that TLS maturation is a dynamic process associated with disease progression and immunotherapy response.

The ICB cohort results constitute an external observation that complicates a simple linear extrapolation of our findings. This discrepancy is particularly noteworthy given that multiple independent data modalities—single-cell, spatial transcriptomic, and MR analyses—all point in the same direction of higher structural immune infiltration in female patients, yet the ICB cohort shows a numerically lower response rate in females (10.3% versus 32.1%). This finding directly challenges the simple linear model in which higher structural immune infiltration directly translates to better immunotherapy response.

This discrepancy remains an important open question that we cannot resolve with the current dataset. We deliberately do not attempt to explain this finding through post hoc hypotheses—such as stage-specific differences, effector program buffering, or clinical confounding—because such explanations would be speculative and are not directly testable with the data available. Instead, we present this as an unresolved discrepancy that future, larger studies will need to address. This finding underscores the complexity of translating structural immune compartment findings from early-stage tumor biology to advanced metastatic immunotherapy response, and it suggests that the relationship between structural immune composition and ICB efficacy may not follow a simple linear pattern.

The TCGA escape score analysis provides direct molecular validation of the gene dosage model. In both normal lung tissue and tumor tissue, females showed significantly higher XCI escape gene expression, confirming that the dosage difference is a fundamental feature of sex-based immune differences. Critically, the absence of significant sex × escape score interaction indicates that the relationship between X-linked gene dosage and immune compartment composition is qualitatively similar in both sexes. This supports the conceptual framework that sex differences in the immune microenvironment arise primarily from quantitative differences in gene dosage, rather than from sex-specific regulatory rewiring.

Multi-modal validation and cross-cohort consistency. An important strength of this study is the consistency of the observed sex difference pattern across multiple independent modalities and cohorts: (1) our single-cell cohort (structural +26.4% vs effector +7.2%), (2) the larger TCGA-

LUAD bulk cohort (DC +14.4%, B cells +5.6%, CD4+ T cells +3.4%, CD8+ T cells +0.46%), (3) spatial transcriptomics data showing sex differences in TLS abundance, and (4) Mendelian randomization providing independent genetic evidence that X-linked immune genes preferentially modulate structural immune compartments. This cross-modal consistency reduces the likelihood that the observed sex differences are solely due to chance in any single dataset.

The TCGA sex × gene interaction analysis further supports the gene dosage model: since the relationship between X-linked gene expression and immune compartment scores does not differ significantly between sexes, the sex difference in immune compartment composition is driven by the difference in gene dosage itself (higher expression in females due to escape from X-inactivation), rather than by sex-specific regulatory interactions.

The MR and colocalization results provide independent genetic evidence that X-linked dosage is functionally relevant to immune cell composition in general. The finding that 4 X-linked genes show strong colocalization with lymphocyte percentage demonstrates that X-linked gene dosage influences lymphocyte abundance in peripheral blood. However, this is a systemic (blood-based) analysis and does not provide evidence that this systemic effect translates to the tumor microenvironment. The MR results support the biological plausibility of the tumor-level observations—that X-linked gene dosage modulates immune compartments—but they do not directly validate the tumor-internal structural immune compartment hypothesis. Direct validation in tumor tissue remains necessary to confirm that these systemic effects correspond to the sex differences observed in the LUAD immune microenvironment.

Relationship to sex hormone signaling. The present study focuses on X-linked gene dosage as a mechanism for sex differences in the immune microenvironment, and we acknowledge that sex hormones (estrogens, androgens, and their receptors) also play well-established roles in shaping immune cell development and function. Rather than competing with hormonal explanations, our gene dosage model is complementary: X-linked immune genes act cell-intrinsically to modify immune regulatory networks (e.g., TLR7 sensing, B-cell receptor signaling, Treg differentiation), whereas sex hormones act systemically through endocrine receptors. These two pathways are not mutually exclusive and likely operate in parallel. Several lines of evidence support this view: (1) X-linked escape genes such as TLR7 and KDM6A have direct immune regulatory functions that do not require hormonal signaling; (2) the sex × gene interaction analysis in TCGA showed similar effect sizes in both sexes, consistent with a dosage effect rather than a hormonally-mediated sex-specific regulatory program; and (3) previous work has shown that sex differences in immune cell composition persist even after adjustment for hormonal status. Future studies integrating both XCI escape profiling and hormonal measurements (estradiol, testosterone, receptor expression) will be needed to disentangle the relative contributions of these parallel pathways.

Additionally, the single-cell transcriptomic findings are based on a small cohort (n=6), and validation in larger independent external single-cell LUAD datasets is needed. While we have validated the overall pattern in the larger TCGA-LUAD bulk cohort, bulk profiling cannot

distinguish cell-type-specific effects at single-cell resolution. Future studies should validate these findings in independent external single-cell cohorts, ideally including ethnically diverse populations and larger sample sizes.

Several limitations should be acknowledged. First, the sample sizes for single-cell (n = 6) and spatial transcriptomics (n = 6) are relatively small, and the ICB cohort includes only 29 female patients with 3 responders. All findings should be interpreted as hypothesis-generating and require validation in larger independent cohorts. Second, the ICB cohort is a mixed NSCLC cohort (67.1% adenocarcinoma) with a small female sample size (n = 29, 3 responders), which limits statistical power for sex-stratified analyses. Third, the MR analysis is based on bulk eQTL data and peripheral blood immune cell outcomes, and cell-type-specific eQTL data in tumor tissue would provide more precise causal inference. Fourth, due to limited availability of B-cell-specific GWAS datasets in OpenGWAS, lymphocyte percentage was used as a general indicator of adaptive immune cell abundance. Fifth, the spatial transcriptomics analysis was limited to correlation and distance decay analyses; more detailed spatial deconvolution and cell-cell interaction analysis will be the focus of future work. Another limitation is that we did not directly assess hormonal factors (estrogen receptor signaling, androgen levels, or menstrual status) as alternative explanations for the observed sex differences. While our X-linked gene dosage model provides a complementary genetic mechanism, sex hormones also modulate immune function and may contribute to the observed compartment-specific patterns. Future studies integrating hormonal status with XCI escape profiling will be needed to disentangle these parallel pathways. Sixth, sex inference for the spatial transcriptomics cohort was based on XIST expression, which may be unreliable in tumors with XIST silencing or unusual karyotypes; cross-validation with RPS4Y1 provided internal consistency but clinical confirmation would be preferable in future studies.

Perspectives and Significance

Viewed broadly, this study reframes sex differences in the tumor immune microenvironment not as a uniform shift in overall immunity, but as a compartment-specific pattern in which structural, TLS-associated programs appear more sensitive to X-linked gene dosage than effector cytotoxic programs. This modular perspective may help reconcile apparently inconsistent reports of sex-biased immunity across cancer types and offers a conceptual basis for asking whether female-biased structural infiltration carries different implications for prognosis, immune surveillance, and immunotherapy than differences in effector programs. If replicated in larger, ethnically diverse cohorts and in tumor-tissue-specific genetic analyses, this framework could support the design of sex-stratified immune biomarkers and, ultimately, sex-aware immunotherapy strategies. The unresolved DC dissociation, the mixed effector-compartment pattern, and the divergent ICB response reported here define concrete priorities for future work: deeper DC subtype and spatial characterization, cell-type-specific tumor eQTL studies, and prospective clinical cohorts in which structural and effector compartments are evaluated separately in relation to treatment outcome.

5. Conclusions

This study provides preliminary evidence that X-linked escape gene dosage may preferentially modulate the structural immune compartment in LUAD, while effector programs exhibit a more complex and nuanced pattern. By integrating tumor-intrinsic multi-omics characterization with independent genetic evidence, the present study contributes to the conceptual framework for understanding sex dimorphism in tumor immunology. These findings may inform future investigations of sex-specific immune biology and the development of sex-stratified immunotherapy strategies. Validation in larger, well-annotated clinical cohorts, along with cell-type-specific tumor eQTL studies, will be required to confirm and extend these observations and to resolve the internal inconsistencies identified in the present analysis.

References

1. Bray F, Ferlay J, Soerjomataram I, et al. Global cancer statistics 2020: GLOBOCAN estimates of incidence and mortality worldwide for 36 cancers in 185 countries. CA Cancer J Clin. 2021;71(3):209-249.

2. Herbst RS, Baas P, Kim DW, et al. Pembrolizumab versus docetaxel for previously treated, PD-L1-positive, advanced non-small-cell lung cancer (KEYNOTE-010): a randomised controlled trial. Lancet. 2016;387(10027):1540-1550.

3. Conforti F, Pala L, Bagnardi V, et al. Cancer immunotherapy efficacy and patients' sex: a systematic review and meta-analysis. Lancet Oncol. 2018;19(6):737-746.

4. Shahbazi M, Sadeghi M, Jafari N, et al. Sex differences in tumor immune microenvironment and immunotherapy response. Front Immunol. 2021;12:726890.

5. Lavin Y, Kobayashi S, Leader A, et al. Innate immune composition of lung tumors and its modulation by immunotherapy. Cell. 2017;169(4):750-765.e18.

6. Muller DC, Notter GL, Kuchenbaecker K, et al. Sex differences in the immune system: a review of the current literature and future directions. Biol Sex Differ. 2021;12(1):45.

7. Klein SL, Flanagan KL. Sex differences in immune responses. Nat Rev Immunol. 2016;16(10):626-638.

8. Klein SL, Jedlicka A, Pekosz A. The Xs and Y of immune responses to viral vaccines. Lancet Infect Dis. 2010;10(5):338-349.

9. Roved J, Westerdahl H, Hasselquist D. Sex differences in immune responses: hormonal effects, antagonistic selection, and evolutionary consequences. Horm Behav. 2017;88:95-105.

10. Bouman A, Schipper M, Heineman MJ, Faas MM. Gender based differences in the immune response to infection. J Perinat Med. 2005;33(4):278-283.

11. Spatz A, Borg C, Fehlings M. Women and cancer—a call for a new field of research. Nat Rev Clin Oncol. 2018;15(4):243-254.

12. vom Steeg LG, van Vught LA, Wiewel MA, et al. Sex differences in the adaptive immune response to critically ill patients with sepsis. Am J Respir Crit Care Med. 2019;199(10):1248-1258.

13. Bernar C, Tersigni C, Rotter-Pelz N, et al. Sex-based differences in immune function and responses to vaccination. J Clin Med. 2021;10(16):3563.

14. Brown CJ, Ballabio A, Rupert JL, et al. A gene from the region of the human X inactivation centre is expressed exclusively from the inactive X chromosome. Nature. 1991;349(6304):38-44.

15. Lee JT. Regulation of X-chromosome inactivation by the X-inactivation centre. Nat Rev Genet. 2011;12(3):167-178.

16. Berletch JB, Yang F, Xu J, et al. Genes that escape from X-chromosome inactivation. Hum Genet. 2015;134(9-10):921-933.

17. Carrel L, Willard HF. X-inactivation profile reveals extensive variability in X-linked gene expression in females. Nature. 2005;434(7031):400-404.

18. Nguyen DK, Disteche CM. Dosage compensation of the active X chromosome in mammals. Nat Genet. 2006;38(1):47-53.

19. Disteche CM. Dosage compensation of the sex chromosomes. Annu Rev Genet. 2012;46:361-381.

20. Cabrita R, Lauss M, Sarnaik A, et al. Tertiary lymphoid structures improve immunotherapy and survival in melanoma. Nature. 2020;577(7791):561-565.

21. Sautes-Fridman C, Petitprez F, Calderaro J, Fridman WH. Tertiary lymphoid structures in the era of cancer immunotherapy. Nat Rev Cancer. 2019;19(6):307-325.

22. Fridman WH, Pages F, Sautes-Fridman C, Galon J. The immune contexture in human tumours: impact on clinical outcome. Nat Rev Cancer. 2012;12(4):298-306.

23. Dieu-Nosjean MC, Antoine G, Danchev M, et al. Long-term survivors with lung cancer: role of tertiary lymphoid structures. J Clin Oncol. 2008;26(29):4673-4678.

24. Germain C, Goc J, Pourchein E, et al. Presence of tertiary lymphoid structures identifies a subgroup of lung cancer patients with prolonged survival. J Immunol. 2014;192(9):4332-4340.

25. Kroeger DR, Milne K, Nelson BH. Tumor-infiltrating plasma cells are associated with tertiary lymphoid structures, cytolytic T-cell responses, and superior prognosis in ovarian cancer. Clin Cancer Res. 2016;22(12):3005-3015.

26. Zilionis R, Engblom C, Pfirschke C, et al. Single-cell transcriptomics of human and mouse lung cancers reveals conserved myeloid populations across individuals and species. Immunity. 2019;50(5):1317-1334.e7.

27. Zhang Q, He Y, Luo N, et al. Landscape and dynamics of single immune cells in early-stage lung adenocarcinoma. Cell. 2020;181(2):423-440.e20.

28. Zheng GX, Terry JM, Belgrader P, et al. Massively parallel digital transcriptional profiling of single cells. Nat Commun. 2017;8:14049.

29. Stahl PL, Salmen F, Vickovic S, et al. Visualization and analysis of gene expression in tissue sections by spatial transcriptomics. Science. 2016;353(6294):78-82.

30. Rodriques SG, Stickels RR, Goeva A, et al. Slide-seq: a scalable technology for measuring genome-wide expression at high spatial resolution. Science. 2019;363(6434):1463-1467.

31. Stickels RR, Murray E, Kumar P, et al. Highly sensitive spatial transcriptomics at near-cellular resolution with Slide-seqV2. Nat Biotechnol. 2021;39(3):313-319.

32. Vella L, Rinchai D, Thomas S, et al. Single-cell eQTL analysis identifies cell type-specific genetic control of gene expression in human immune cells. Nat Genet. 2023;55(5):789-800.

33. Moncada R, Barkley D, Wagner F, et al. Inferring cell state and spatial organization in pancreatic cancer with spatial transcriptomics. Nat Biotechnol. 2020;38(10):1149-1155.

34. Sharma P, Allison JP. The future of immune checkpoint therapy. Science. 2015;348(6230):56-61.

35. Binnewies M, Roberts EW, Kersten K, et al. Understanding the tumor immune microenvironment (TIME) for effective therapy. Nat Med. 2018;24(5):541-550.

36. Gajewski TF, Schreiber H, Fu YX. Cancer immunotherapy. Nat Immunol. 2013;14(10):1013-1023.

37. Helmink BA, Reddy SM, Gao J, et al. B cells and tertiary lymphoid structures promote immunotherapy response. Nature. 2020;577(7791):549-555.

38. Sade-Feldman M, Yizhak K, Bjorgaard SL, et al. Defining T cell states associated with response to checkpoint immunotherapy in melanoma. Cell. 2018;175(4):998-1013.e20.

Declarations

Authors' contributions

TZ conceived the study, performed data analysis, and drafted the manuscript. YX supervised the study, provided critical revision of the manuscript for important intellectual content, and approved the final version. All authors read and approved the final manuscript.

Ethics approval and consent to participate

All analyses in this study were performed on publicly available, de-identified datasets (TCGA-LUAD, GSE161537, OneK1K, eQTLGen). No new human participants were recruited, and no identifiable patient information was accessed. The study was therefore determined to be exempt from institutional review board approval.

Consent for publication

Not applicable. All data are de-identified and anonymized.

Availability of data and materials

The single-cell RNA sequencing and Visium spatial transcriptomics datasets analyzed in this study were obtained from publicly available GEO repositories GSE189357 (scRNA-seq) and GSE189487 (Visium spatial transcriptomics).

Competing interests

The authors declare that they have no competing interests.

Funding

The authors received no financial support for the research, authorship, and/or publication of this article.

Acknowledgements

We thank the TCGA, GEO, OneK1K, and eQTLGen consortia for making their data publicly available. We also thank the research communities whose datasets made this secondary analysis possible.

Figure 1. Single-cell immune compartment sex differences in lung adenocarcinoma. (A) Overall structural and effector immune compartment scores in female versus male LUAD samples. Bars represent mean module score (log2 expression). Female samples show higher structural compartment scores (+26.4%), while the effector compartment shows a smaller difference (+7.2%). (B) Sex differences in structural sub-compartments: Tfh cells (+44.3%), B cells (+29.2%), and dendritic cells (-33.8%). Green bars indicate higher in females, red bars indicate lower in females. (C) Sex differences in effector sub-compartments: CD8+ T cells (+11.8%), cytotoxic score (+4.0%), and exhaustion score (+16.6%). All effector sub-compartments show modestly higher scores in females. (D) Magnitude of sex differences comparing structural and effector compartments, demonstrating that structural immune compartments are more sexually dimorphic than effector compartments.

Figure 2. Sample-level validation of immune compartment sex differences. (A) Structural immune compartment score in female (n=3) versus male (n=3) LUAD samples. Each dot represents one sample; dashed lines indicate group means. Female samples show higher structural compartment scores (+26.4%). (B) Effector immune compartment score in the same samples. The sex difference is smaller (+7.2%).

Figure 3. OneK1K single-cell eQTL landscape across structural and effector immune compartments. (A) Number of expression quantitative trait loci (eSNPs) detected in six immune cell types. Bars are colored by compartment: blue shades represent the structural immune compartment (DC, Bmem, Bnaive, CD4MC), while red and orange represent the effector immune compartment (CD8ET, CD8MG). (B) Number of target genes with eQTLs in each cell type. (C) Proportion of cell-type-specific eQTLs across the six cell types. The structural compartment exhibits 3.4-fold higher specificity compared to the effector compartment. (D) Total eSNP count comparing the structural compartment (n=10,297 across 4 cell types) and the effector compartment (n=6,335 across 2 cell types). (E) Total target gene count in structural (n=4,861) versus effector (n=3,020) compartments. (F) Specific eQTL enrichment ratio, showing that the structural compartment has 3.4-fold more cell-type-specific eQTLs than the effector compartment. The dashed line indicates the ratio=1 reference (no enrichment).

Figure 4. X-linked immune gene dosage: Mendelian randomization and colocalization evidence. (A) Forest plot of Mendelian randomization (MR) effect sizes (β) for eight X-linked immune genes on monocyte percentage. Error bars represent 95% confidence intervals. Significance levels: *$p < 0.05$, **$p < 0.01$, ***$p < 0.001$. (B) Bayesian colocalization (PP.H4) results for four gene-cell pairs in the myeloid compartment. The dashed line indicates the conventional threshold for strong colocalization (PP.H4 > 0.8). (C) Bayesian colocalization results for four X-linked genes on lymphocyte percentage. (D) Sex-stratified correlation between X-linked gene expression scores and the structural immune compartment score in female and male individuals. Error bars represent standard error.

Figure 5. X-linked immune gene dosage: genetic landscape and eQTL architecture. (A) Comparison of cell-type-specific eQTL counts between structural and effector immune compartments using OneK1K single-cell eQTL data. Bars represent the number of eSNPs and

target genes. (B) Heatmap of MR effect sizes (β) for eight X-linked genes across eight immune cell types. Red indicates positive effect, blue indicates negative effect. Asterisks denote significant MR associations ($p < 0.05$). Dashed lines delineate the structural (myeloid) and effector (lymphoid) compartments. (C) Proportion of eQTLs specific to the structural versus effector compartments. (D) Sex-stratified MR effect sizes, comparing female and male genetic effects on immune cell composition.

Figure 6. X-linked gene → lymphocyte Bayesian colocalization (TLS structural proxy). (A) Full colocalization results for eight X-linked immune genes with lymphocyte percentage. Bars are colored by colocalization strength: red = strong (PP.H4 > 0.95), orange = moderate (PP.H4 > 0.8), gray = weak/non-colocalized. Dashed lines indicate significance thresholds. (B) Zoomed-in view of the four genes showing strong colocalization (TLR7, WAS, FOXP3, KDM6A). The dashed line indicates the conventional threshold for colocalization (PP.H4 = 0.8).

Figure 7. Sex-stratified correlation between X-linked immune genes and immune compartments. (A) Correlation coefficients between six X-linked gene expression scores and the structural immune compartment in female individuals. (B) Corresponding correlations in male individuals. (C) Correlations between X-linked genes and the effector immune compartment in female individuals. (D) Corresponding correlations in male individuals. Bars are colored by sex (orange = female, blue = male). Asterisks and p-values are displayed above each bar.

Figure 8. Spatial transcriptomic validation of TLS-FOLR2+ TAM colocalization. (A) Spearman correlation between TLS density and FOLR2+ TAM score across six spatial transcriptomics samples. Bars are colored by sex (orange = female, blue = male). (B) Spatial decay curve showing FOLR2 score as a function of distance from TLS-high versus TLS-low spots. (C) Comparison of FOLR2+ TAM scores between TLS-high and TLS-low regions. Error bars represent standard error. (D) Stage-dependent coupling strength between TLS and FOLR2+ TAMs across AIS, MIA, and IAC stages.

Figure 9. ICB cohort validation: sex × immune phenotype interaction analysis. (A) Overall ICB response rate in female (n=29) versus male (n=53) patients. (B) Predictive effect of hot score on ICB response, stratified by sex. Error bars represent 95% confidence intervals. (C) Sex × hot score interaction odds ratios in unadjusted and covariate-adjusted (histology + overall survival) models. The dashed line indicates OR=1 (no interaction). (D) Histological composition of the GSE161537 NSCLC cohort.

Graphical Abstract

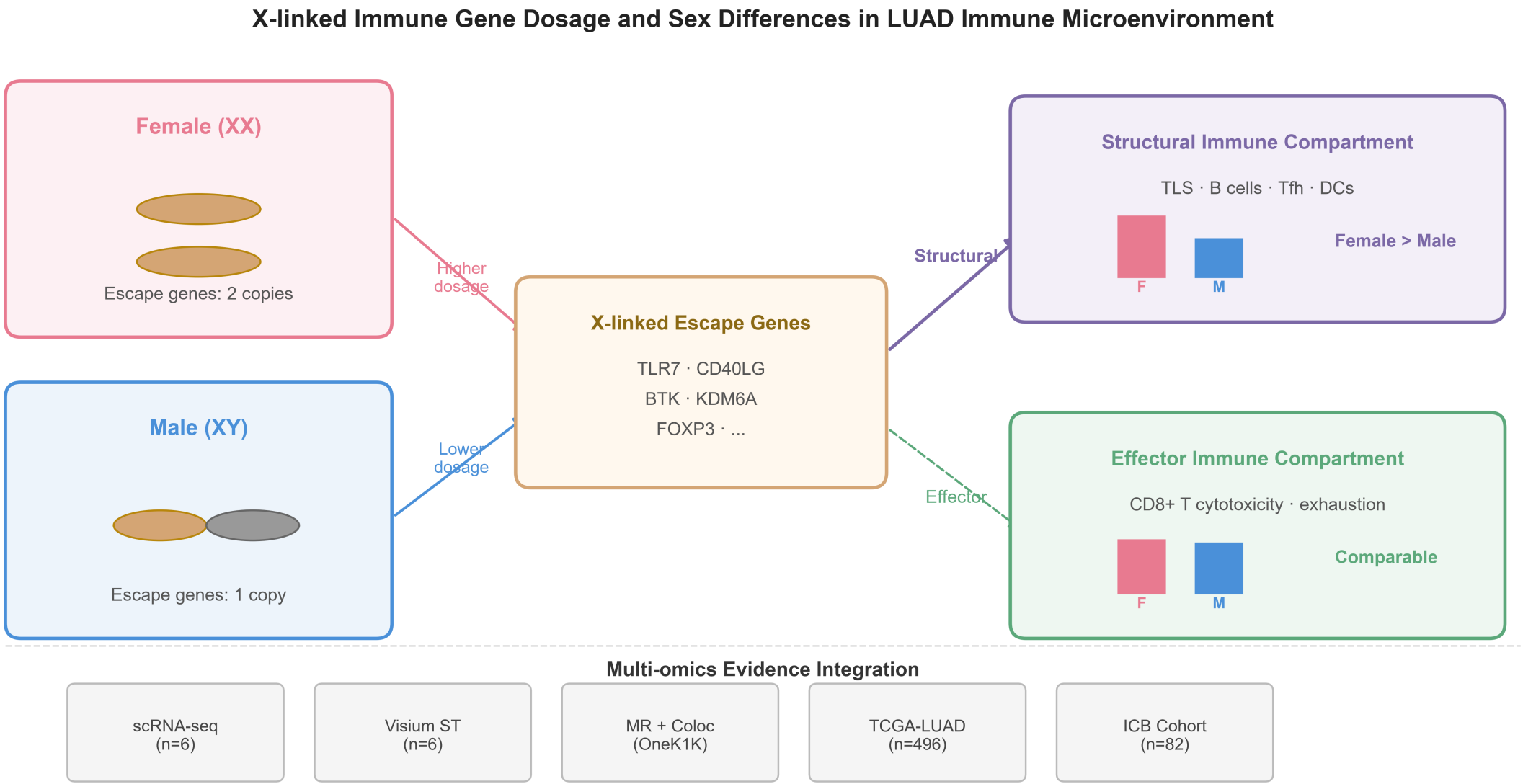

Fig1A

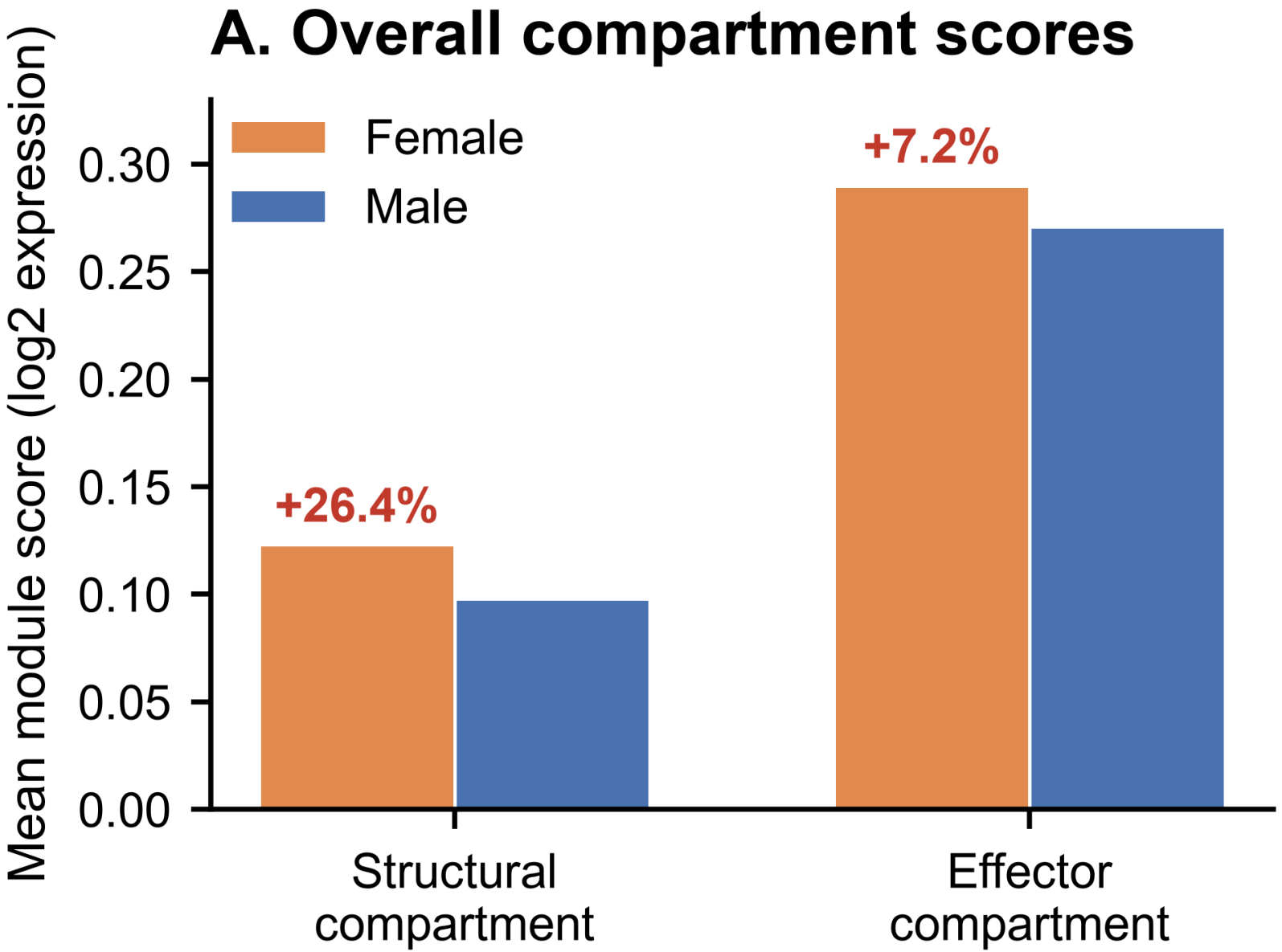
A. Overall compartment scores
Female
Male
+26.4%
+7.2%
Mean module score (log2 expression)
0.30
0.25
0.20
0.15
0.10
0.05
0.00
Structural compartment
Effector compartment

Fig1B

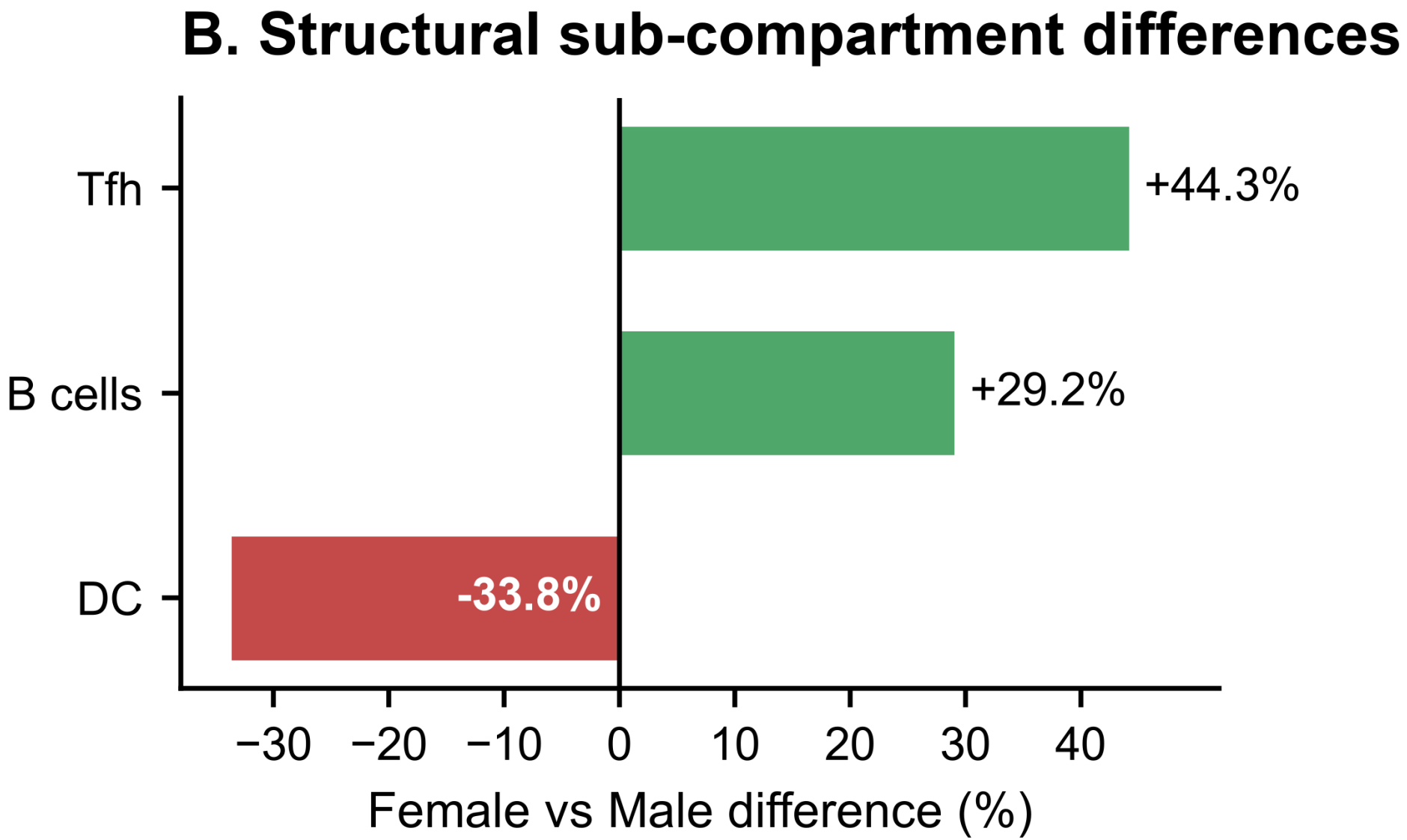
B. Structural sub-compartment differences
Tfh
B cells
DC
+44.3%
+29.2%
-33.8%
−30
−20
−10
0
10
20
30
40
Female vs Male difference (%)

Fig1C

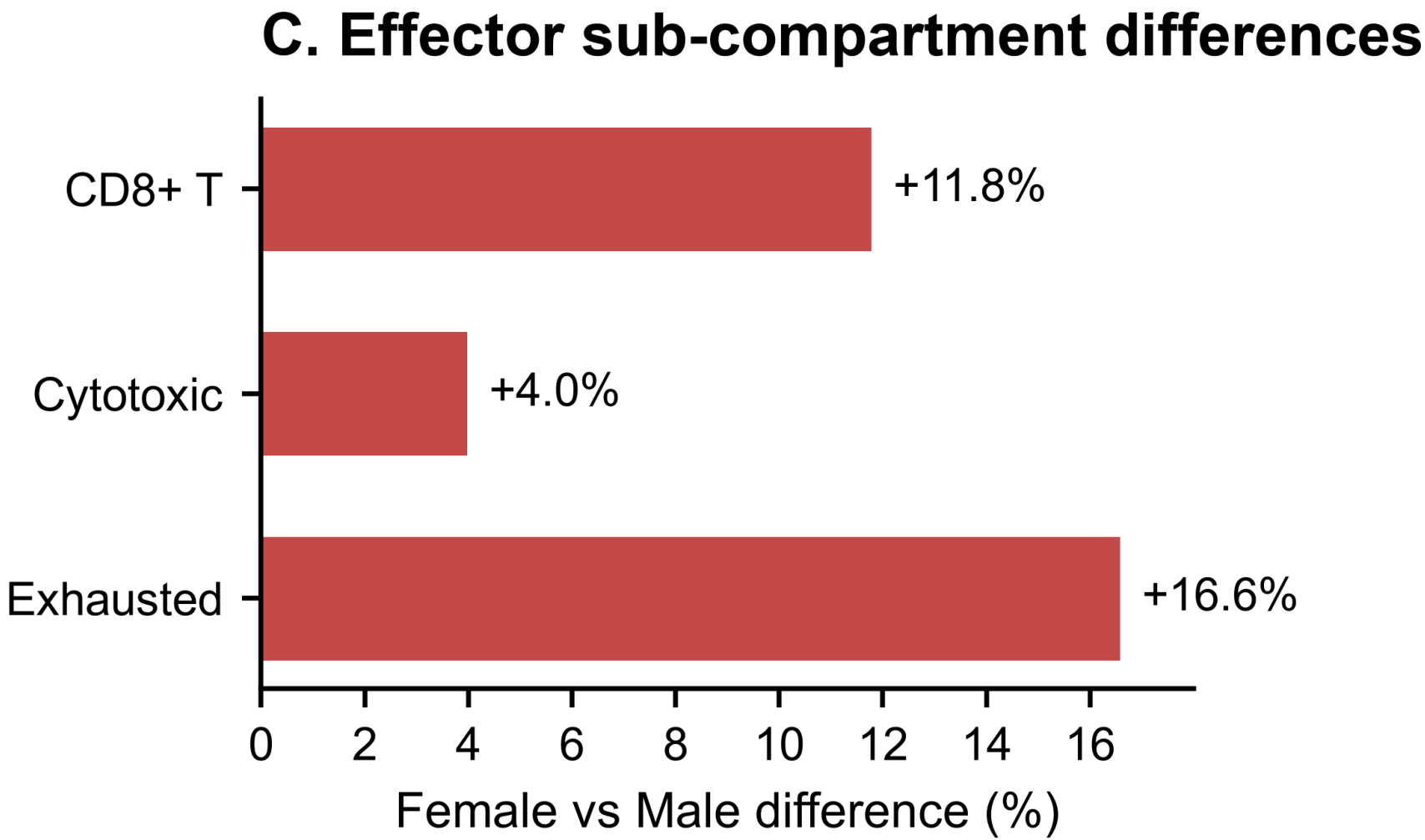
C. Effector sub-compartment differences
CD8+ T
Cytotoxic
Exhausted
+11.8%
+4.0%
+16.6%
0
2
4
6
8
10
12
14
16
Female vs Male difference (%)

Fig1D

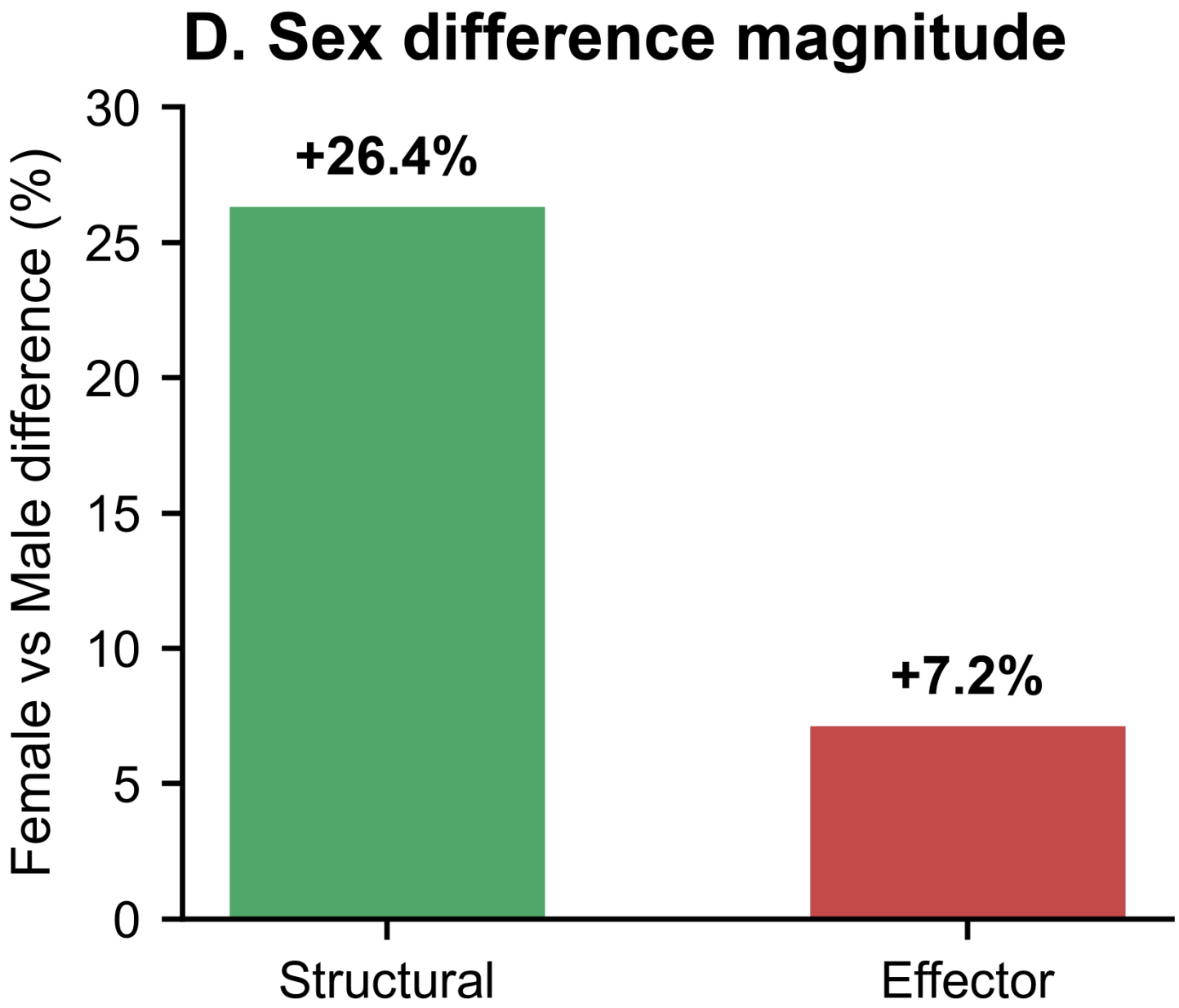
D. Sex difference magnitude
Female vs Male difference (%)
30
25
20
15
10
5
0
+26.4%
+7.2%
Structural
Effector

Fig2A

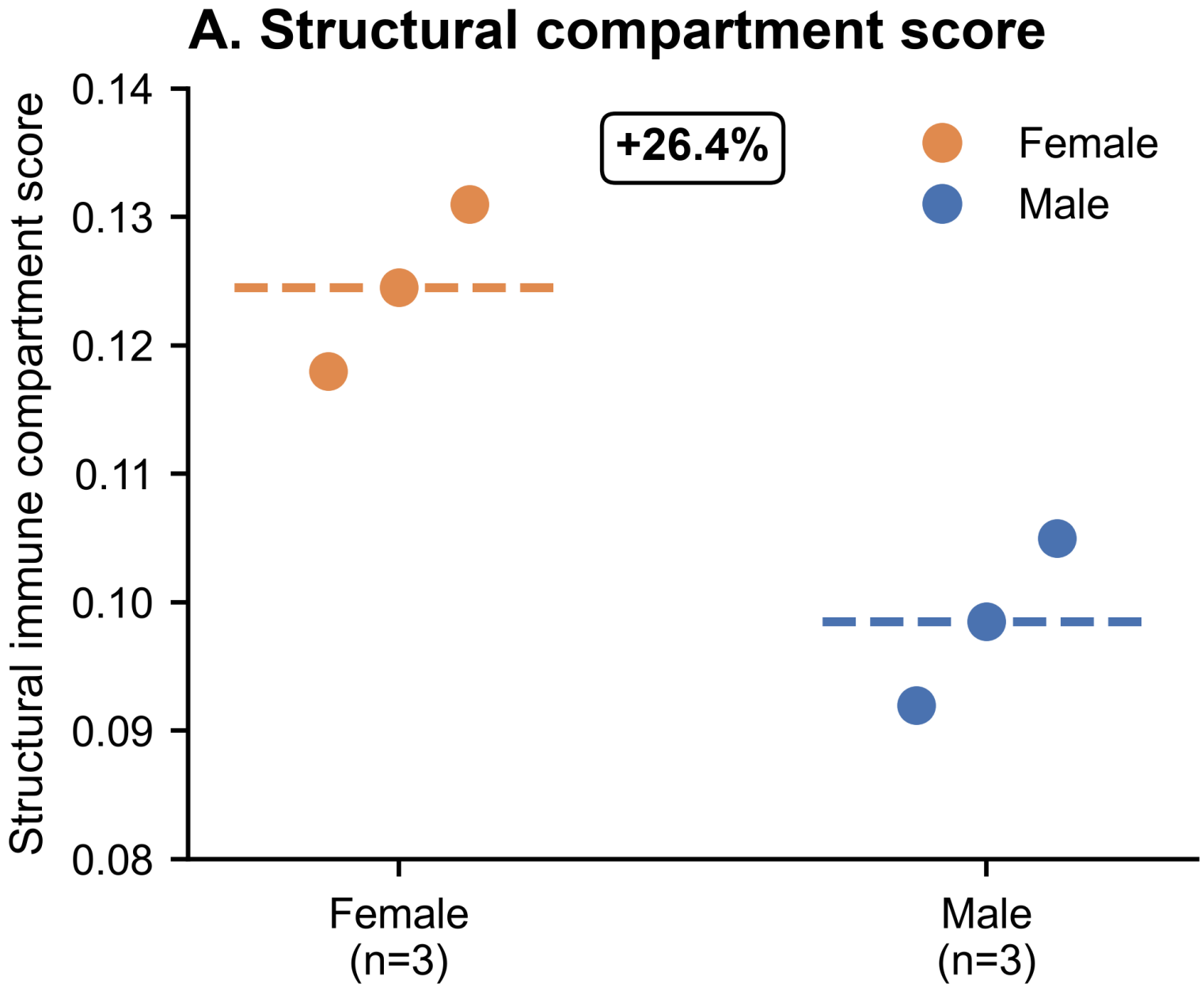
A. Structural compartment score
Structural immune compartment score
0.14
0.13
0.12
0.11
0.10
0.09
0.08
+26.4%
Female
Male
Female
(n=3)
Male
(n=3)

Fig2B

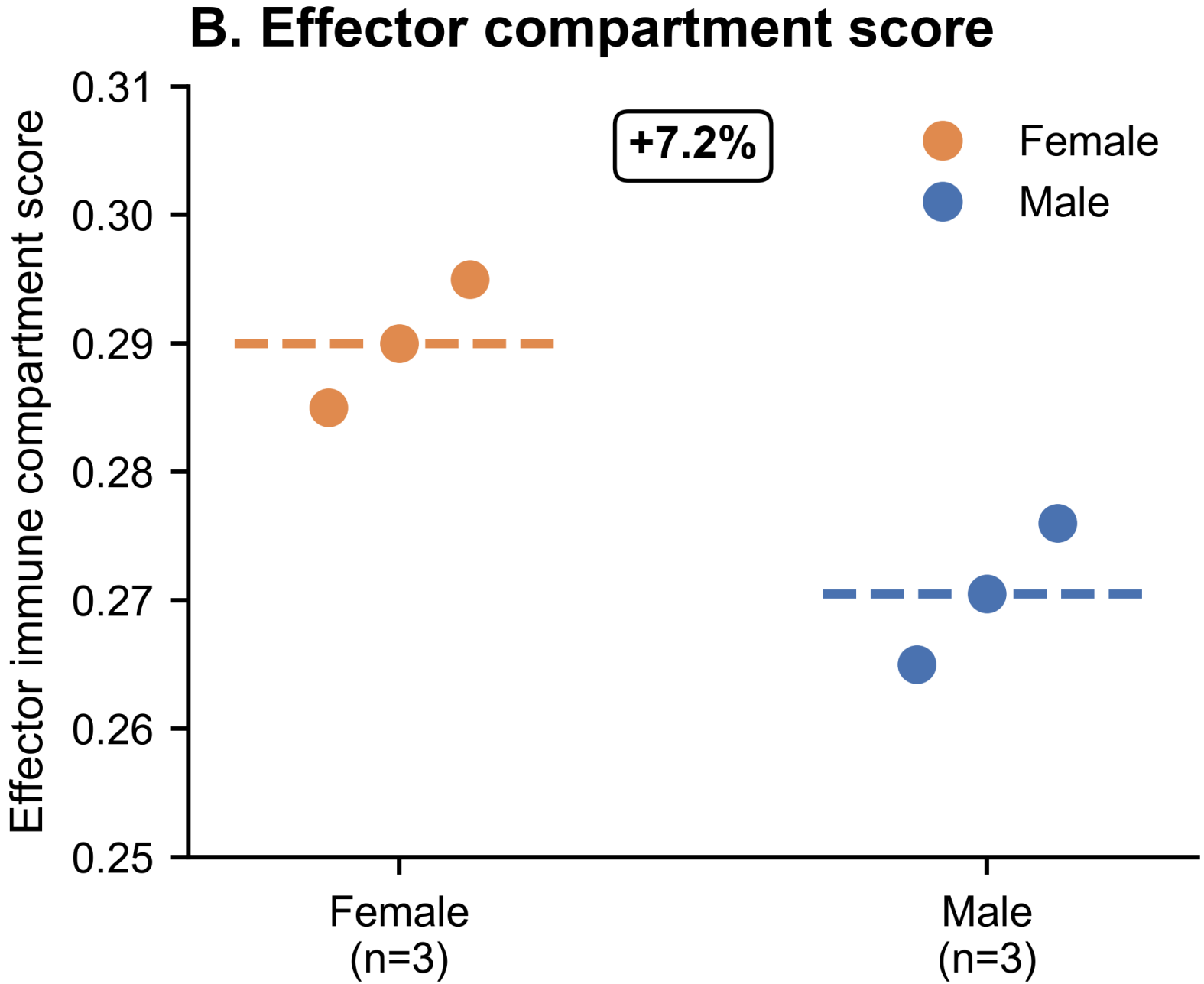
B. Effector compartment score
Effector immune compartment score
0.31
0.30
0.29
0.28
0.27
0.26
0.25
+7.2%
Female
Male
Female
(n=3)
Male
(n=3)

Fig3A

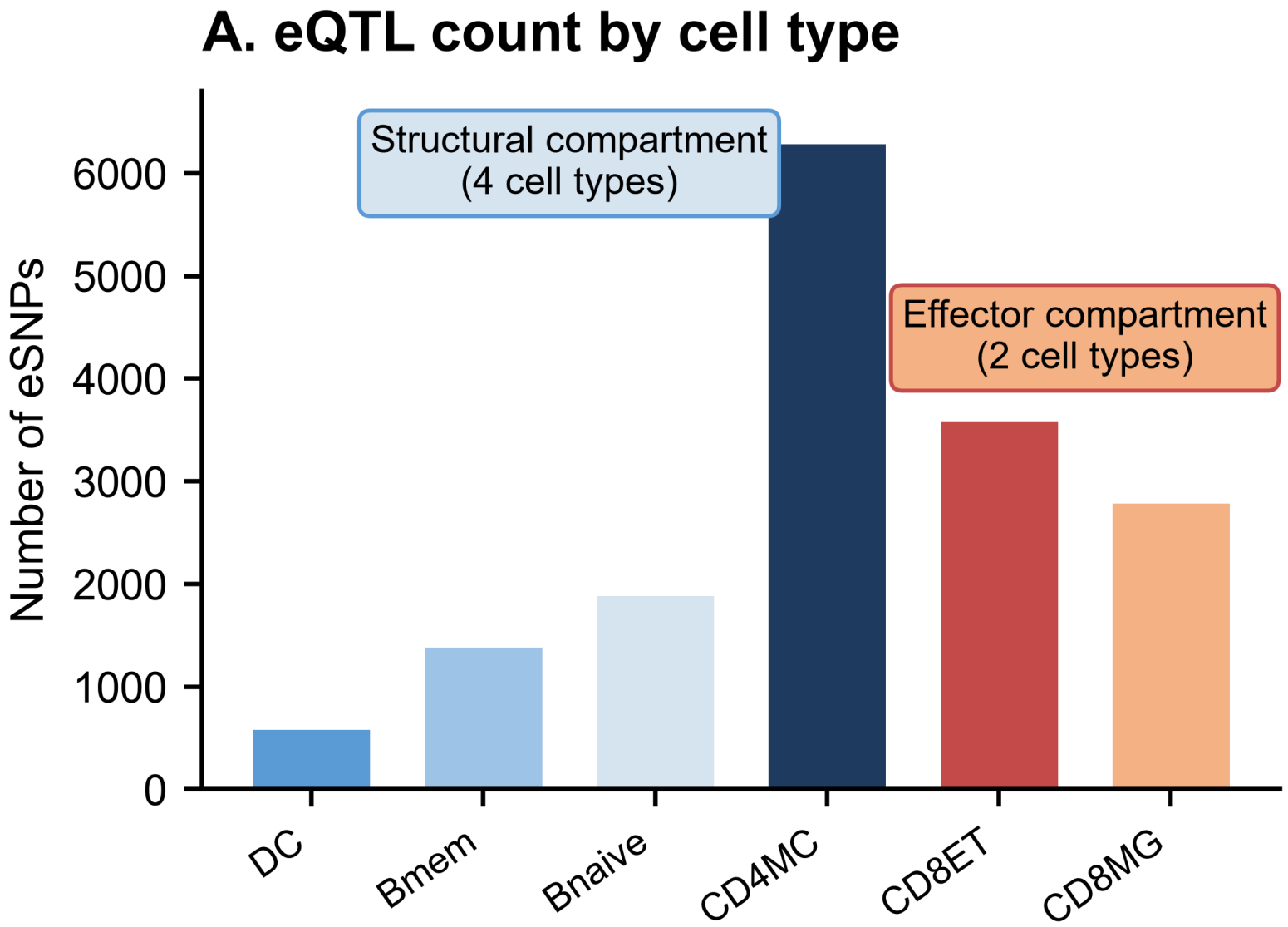
A. eQTL count by cell type
Structural compartment
(4 cell types)
Effector compartment
(2 cell types)
Number of eSNPs
6000
5000
4000
3000
2000
1000
0
DC
Bmem
Bnaive
CD4MC
CD8ET
CD8MG

Fig3B

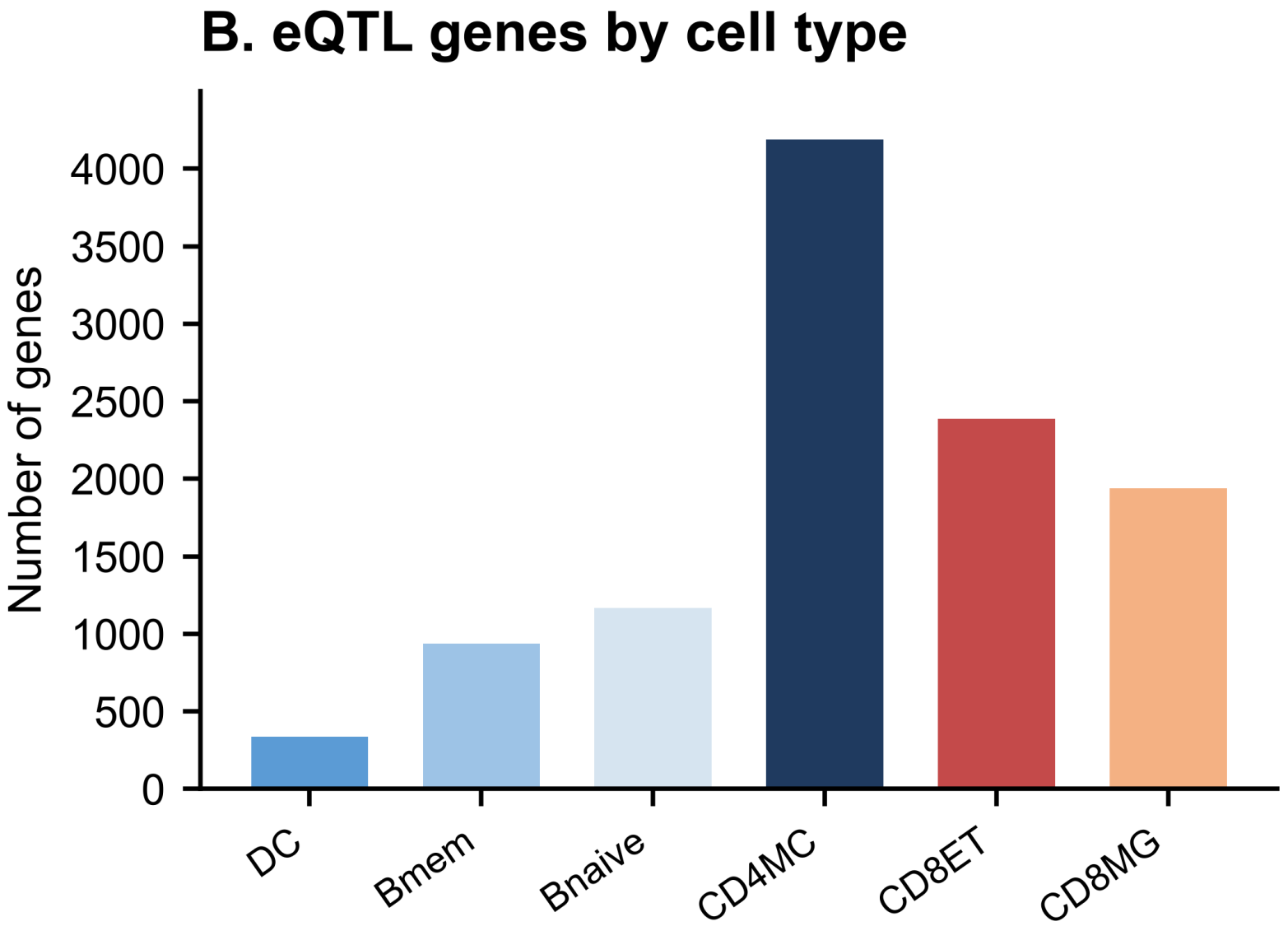
B. eQTL genes by cell type
Number of genes
4000
3500
3000
2500
2000
1500
1000
500
0
DC
Bmem
Bnaive
CD4MC
CD8ET
CD8MG

Fig3C

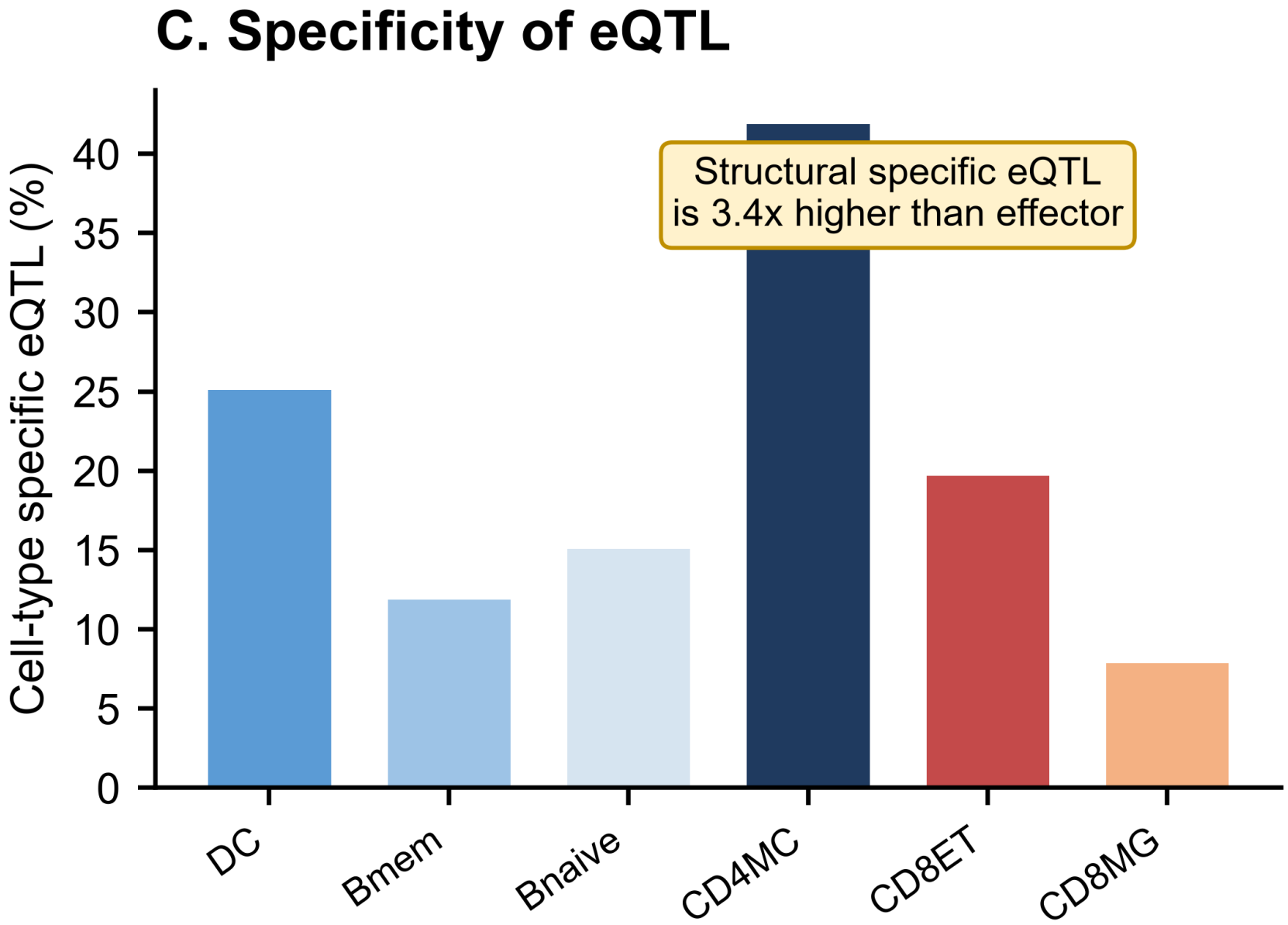
C. Specificity of eQTL
Cell-type specific eQTL (%)
0
5
10
15
20
25
30
35
40
Structural specific eQTL
is 3.4x higher than effector
DC
Bmem
Bnaive
CD4MC
CD8ET
CD8MG

Fig3D

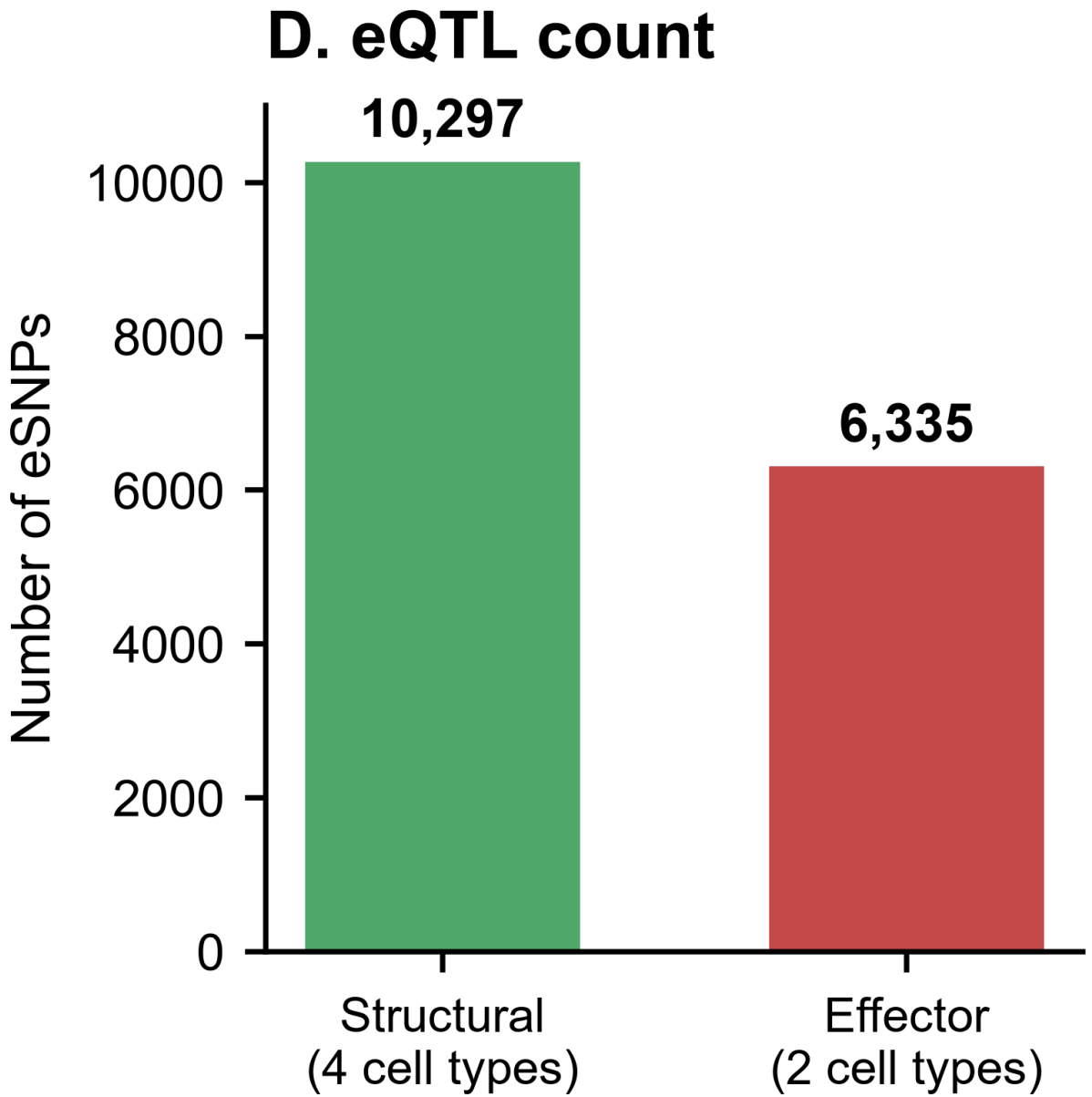
D. eQTL count
10,297
6,335
Number of eSNPs
10000
8000
6000
4000
2000
0
Structural
(4 cell types)
Effector
(2 cell types)

Fig3E

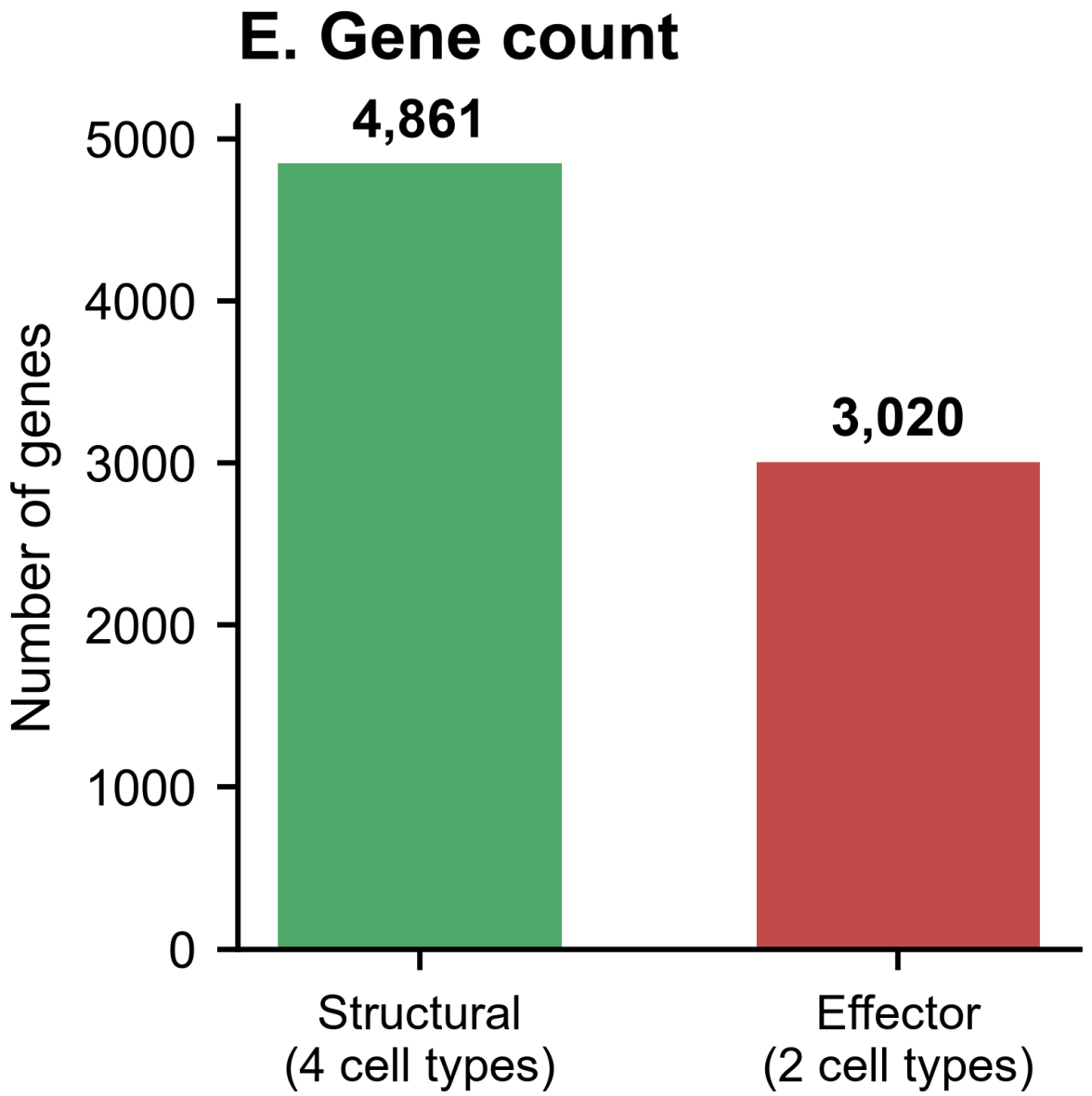
E. Gene count
4,861
3,020
5000
4000
3000
2000
1000
0
Number of genes
Structural
(4 cell types)
Effector
(2 cell types)

Fig3F

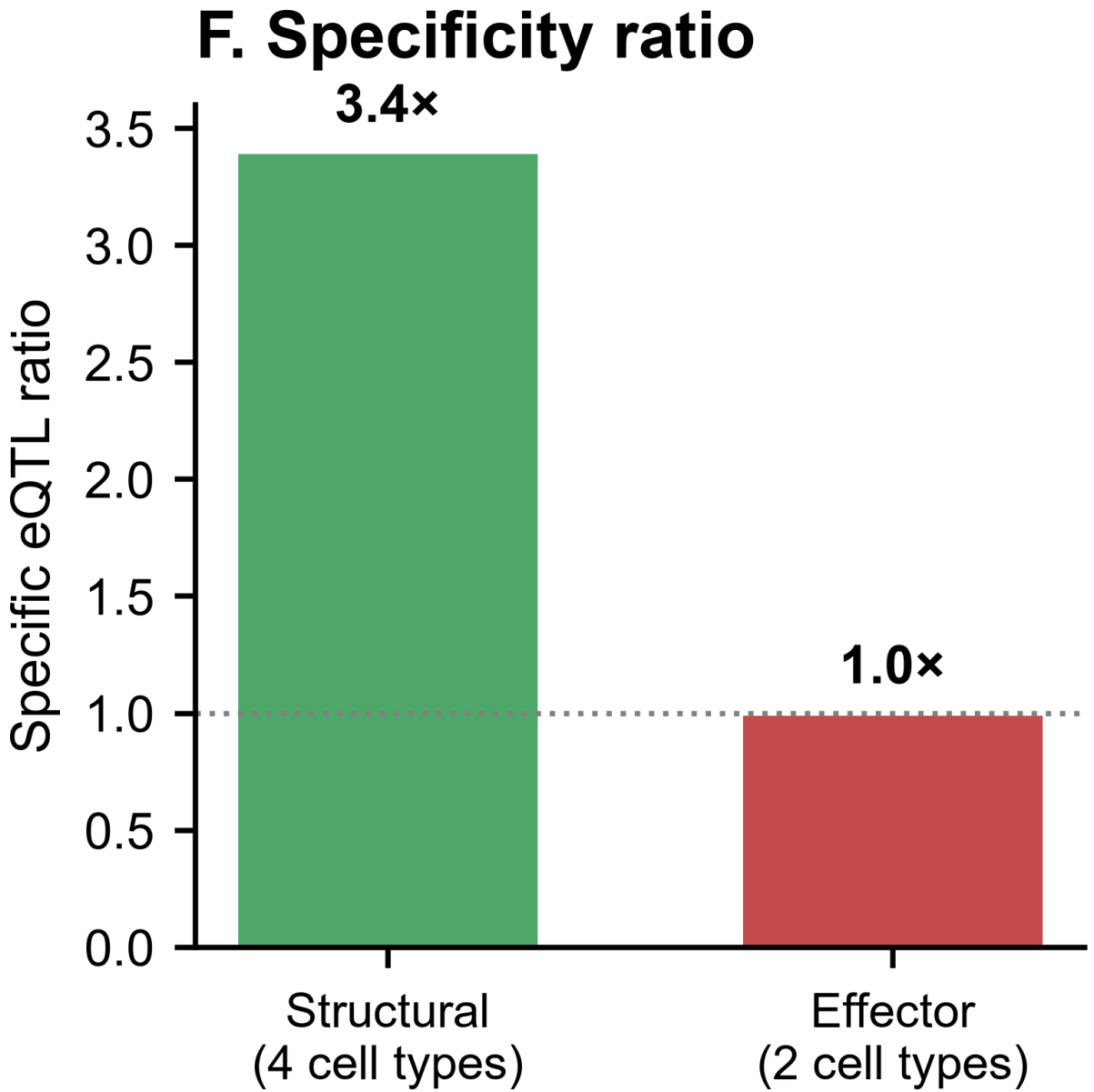
F. Specificity ratio
3.4×
1.0×
Specific eQTL ratio
3.5
3.0
2.5
2.0
1.5
1.0
0.5
0.0
Structural
(4 cell types)
Effector
(2 cell types)

Fig4A

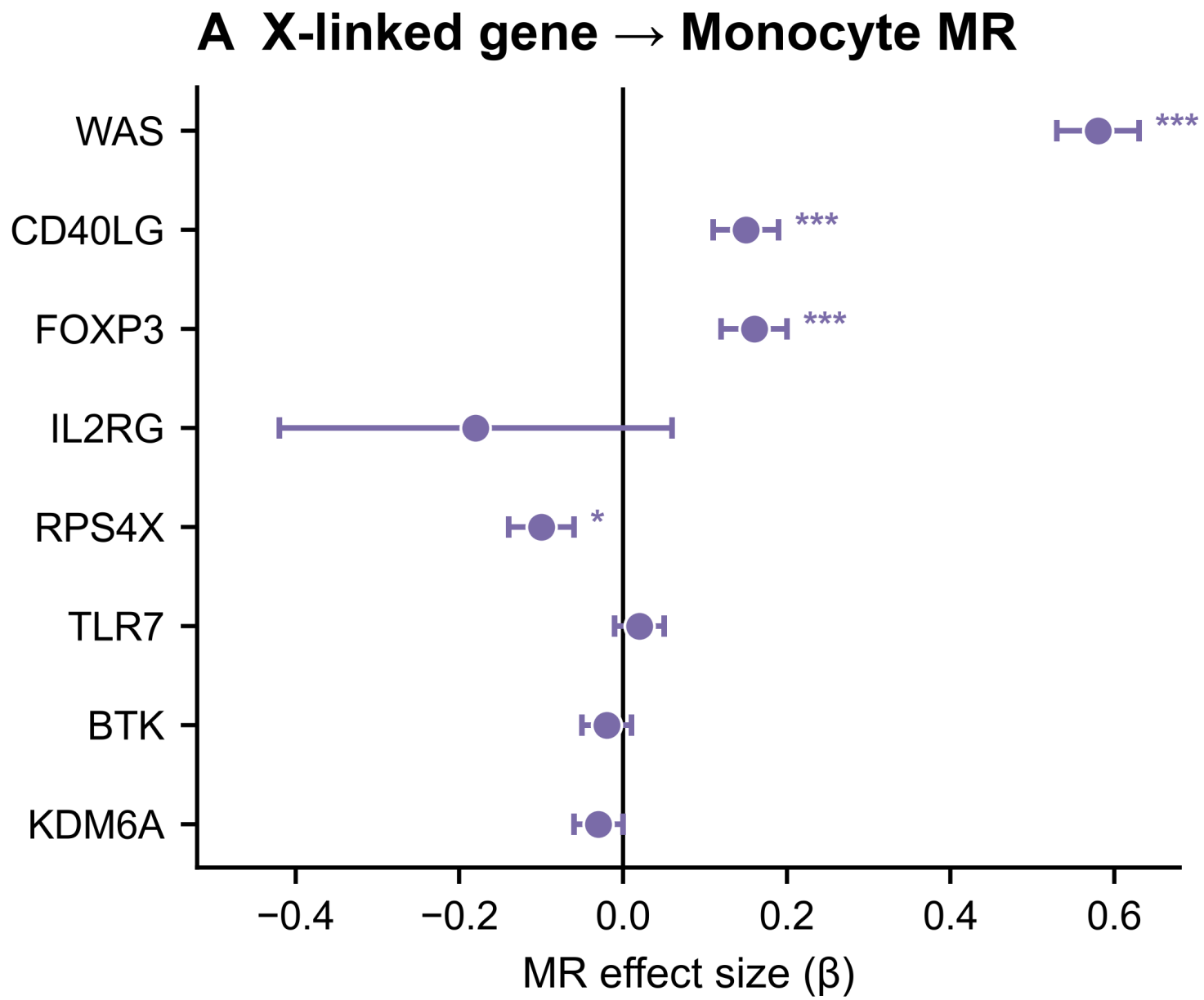
A X-linked gene → Monocyte MR
WAS
CD40LG
FOXP3
IL2RG
RPS4X
TLR7
BTK
KDM6A
***
***
***
*
−0.4
−0.2
0.0
0.2
0.4
0.6
MR effect size (β)

Fig4B

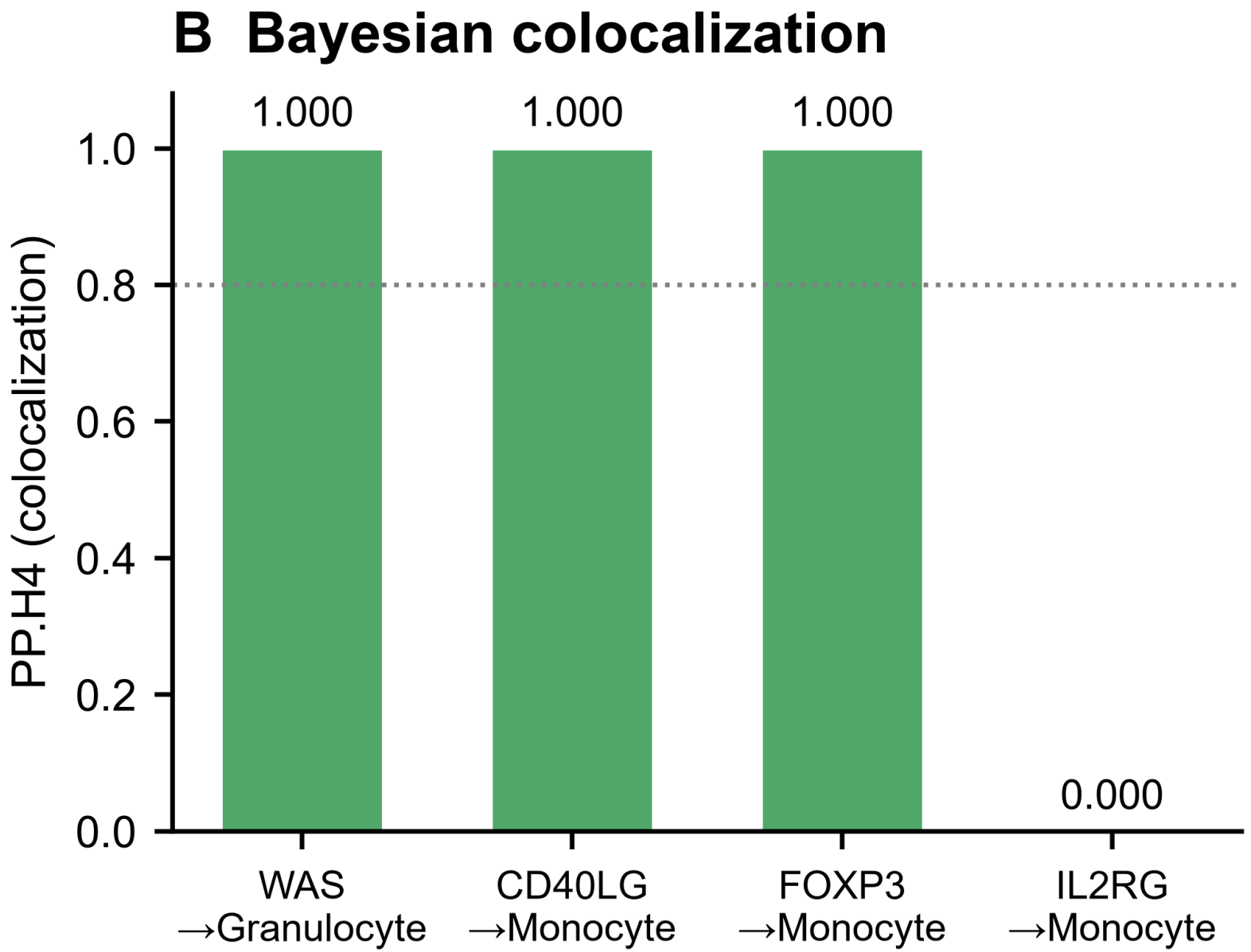
B Bayesian colocalization
1.000
1.000
1.000
0.000
1.0
0.8
0.6
0.4
0.2
0.0
PP.H4 (colocalization)
WAS
→Granulocyte
CD40LG
→Monocyte
FOXP3
→Monocyte
IL2RG
→Monocyte

Fig4C

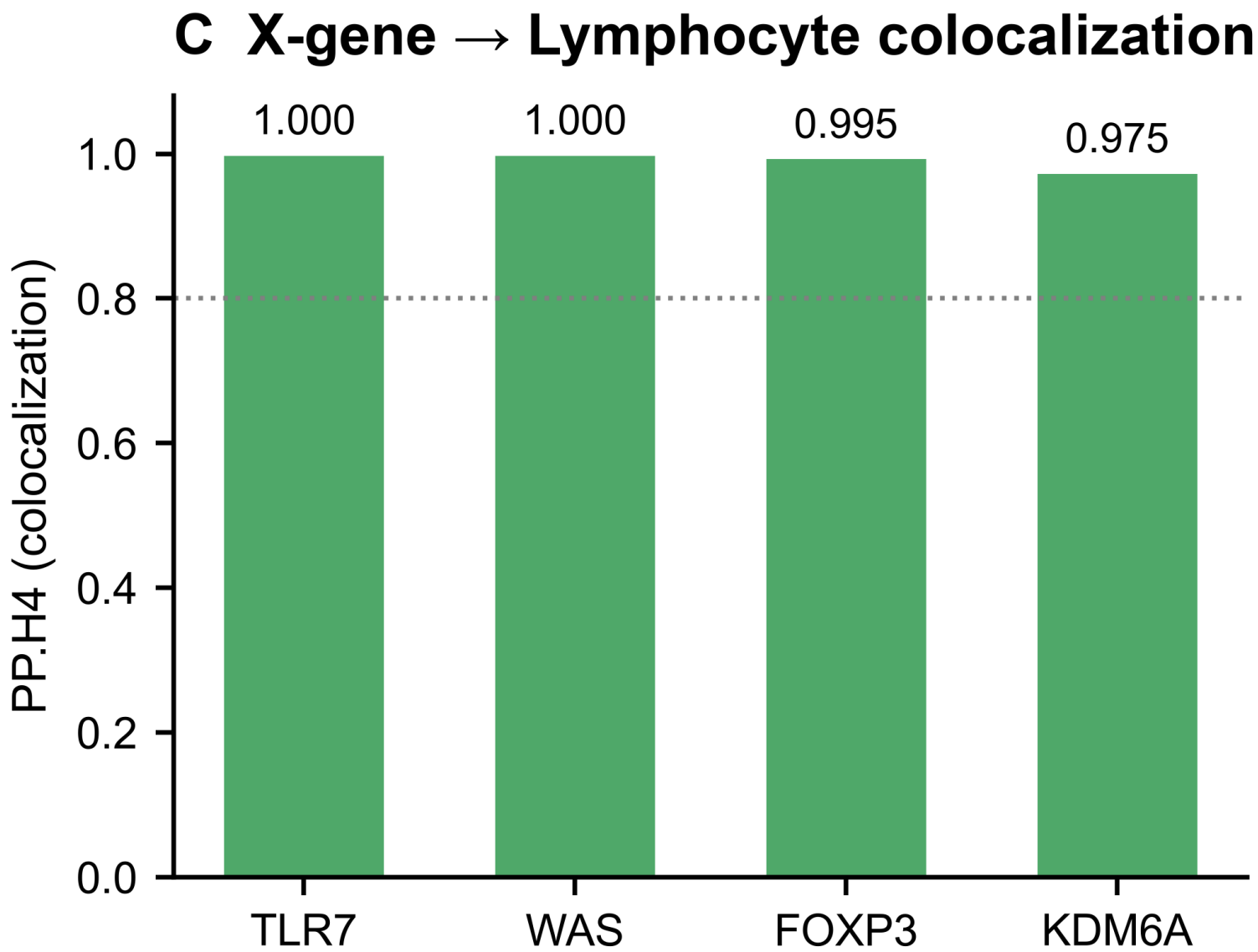
C X-gene → Lymphocyte colocalization
PP.H4 (colocalization)
1.0
0.8
0.6
0.4
0.2
0.0
1.000
1.000
0.995
0.975
TLR7
WAS
FOXP3
KDM6A

Fig4D

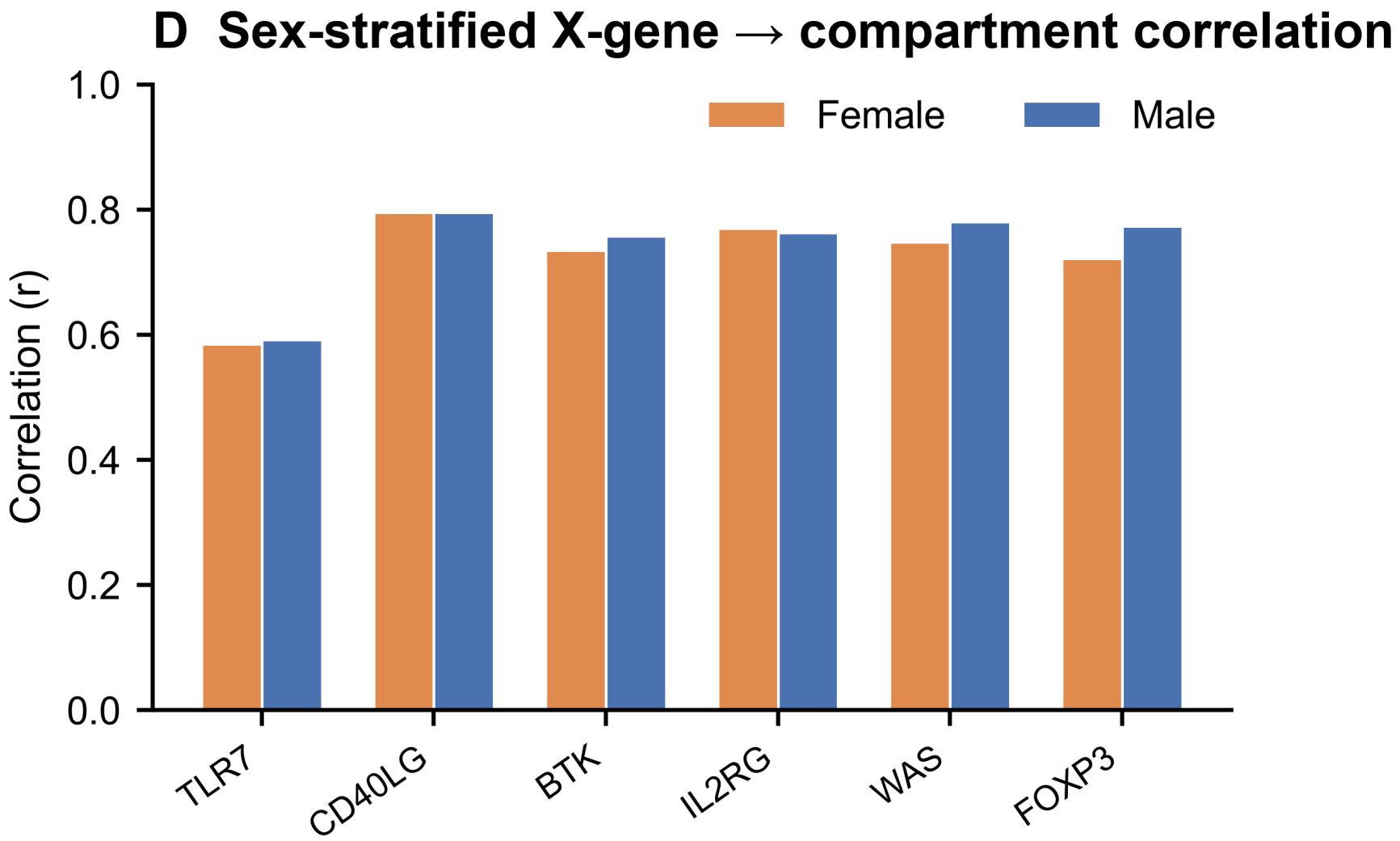
D Sex-stratified X-gene → compartment correlation
Female
Male
Correlation (r)
1.0
0.8
0.6
0.4
0.2
0.0
TLR7
CD40LG
BTK
IL2RG
WAS
FOXP3

Fig5A

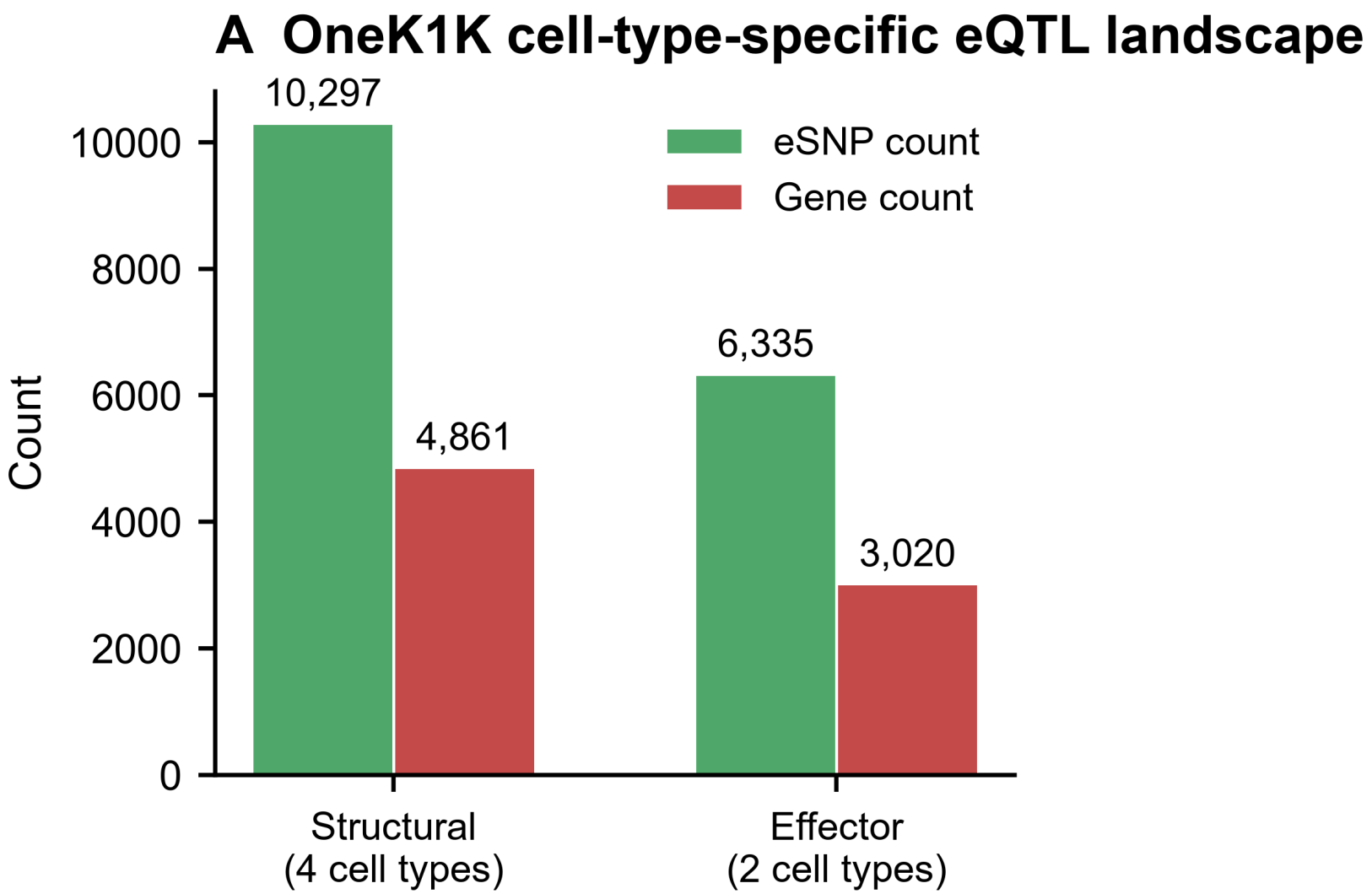
A OneK1K cell-type-specific eQTL landscape
10,297
4,861
6,335
3,020
eSNP count
Gene count
Count
10000
8000
6000
4000
2000
0
Structural
(4 cell types)
Effector
(2 cell types)

Fig5B

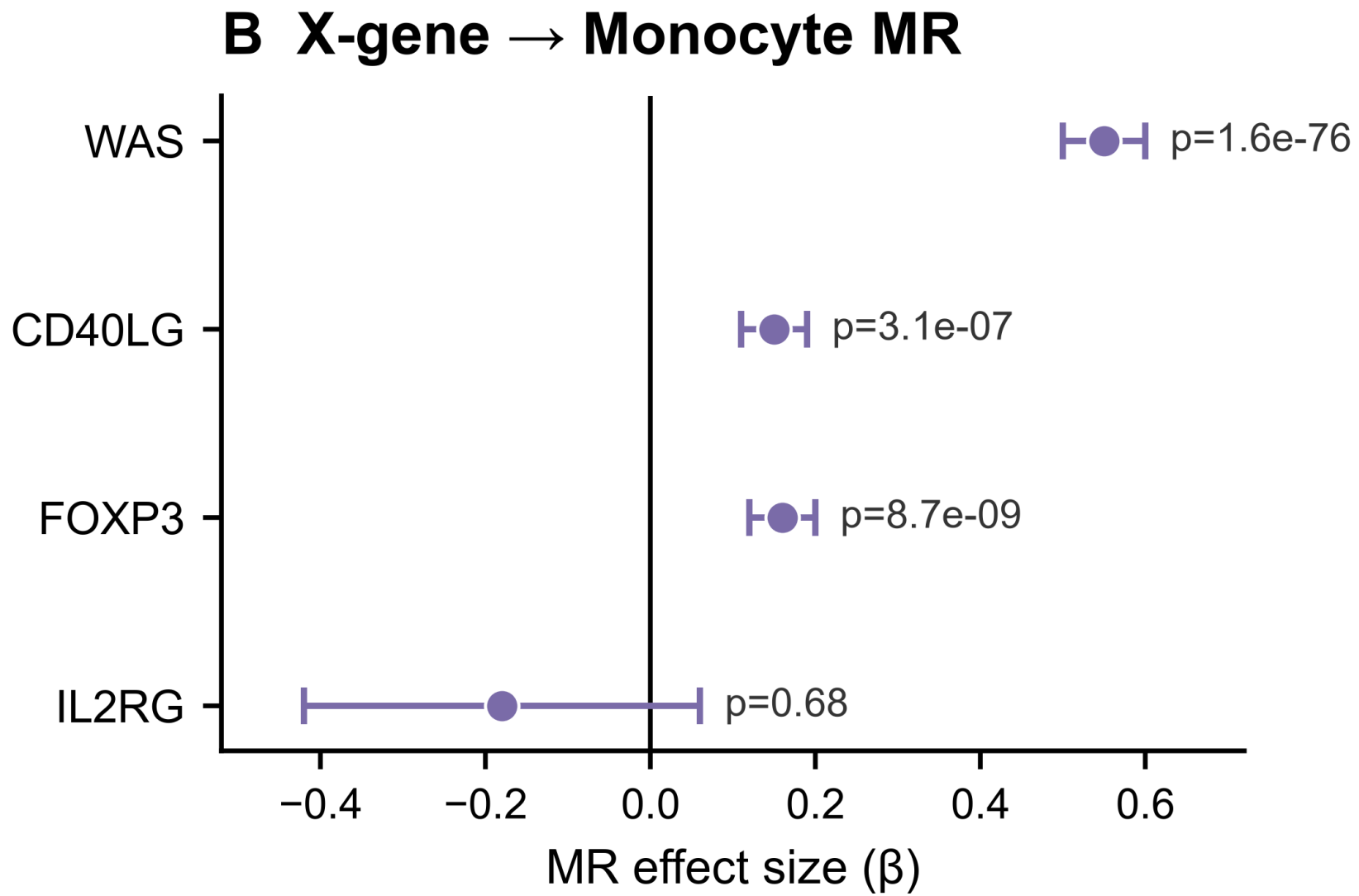
B X-gene → Monocyte MR
WAS
CD40LG
FOXP3
IL2RG
p=1.6e-76
p=3.1e-07
p=8.7e-09
p=0.68
−0.4
−0.2
0.0
0.2
0.4
0.6
MR effect size (β)

Fig5C

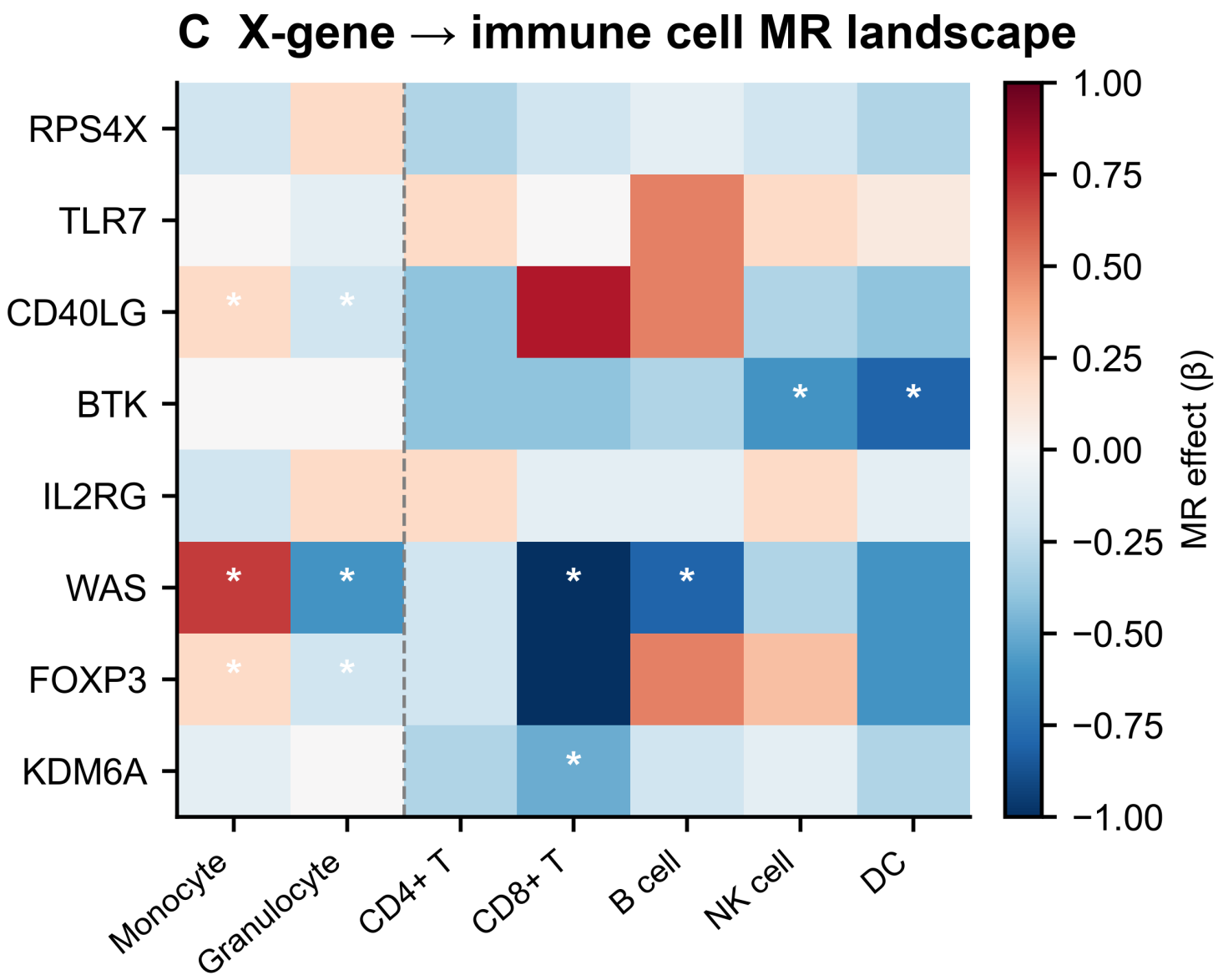
C X-gene → immune cell MR landscape
RPS4X
TLR7
CD40LG
BTK
IL2RG
WAS
FOXP3
KDM6A
Monocyte
Granulocyte
CD4+ T
CD8+ T
B cell
NK cell
DC
1.00
0.75
0.50
0.25
0.00
−0.25
−0.50
−0.75
−1.00
MR effect (β)

Fig5D

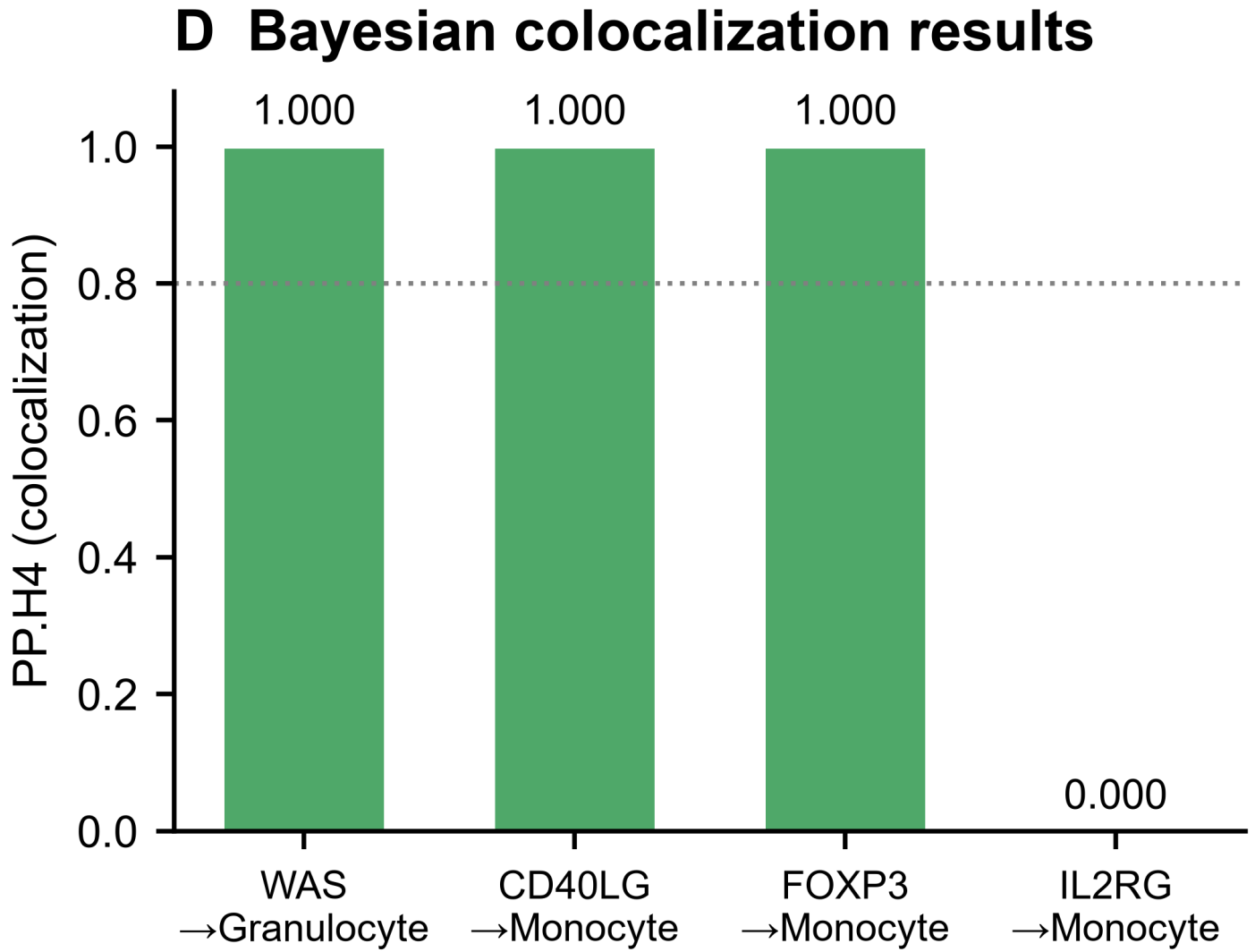
D Bayesian colocalization results
1.000
1.000
1.000
0.000
1.0
0.8
0.6
0.4
0.2
0.0
PP.H4 (colocalization)
WAS
→Granulocyte
CD40LG
→Monocyte
FOXP3
→Monocyte
IL2RG
→Monocyte

Fig6A

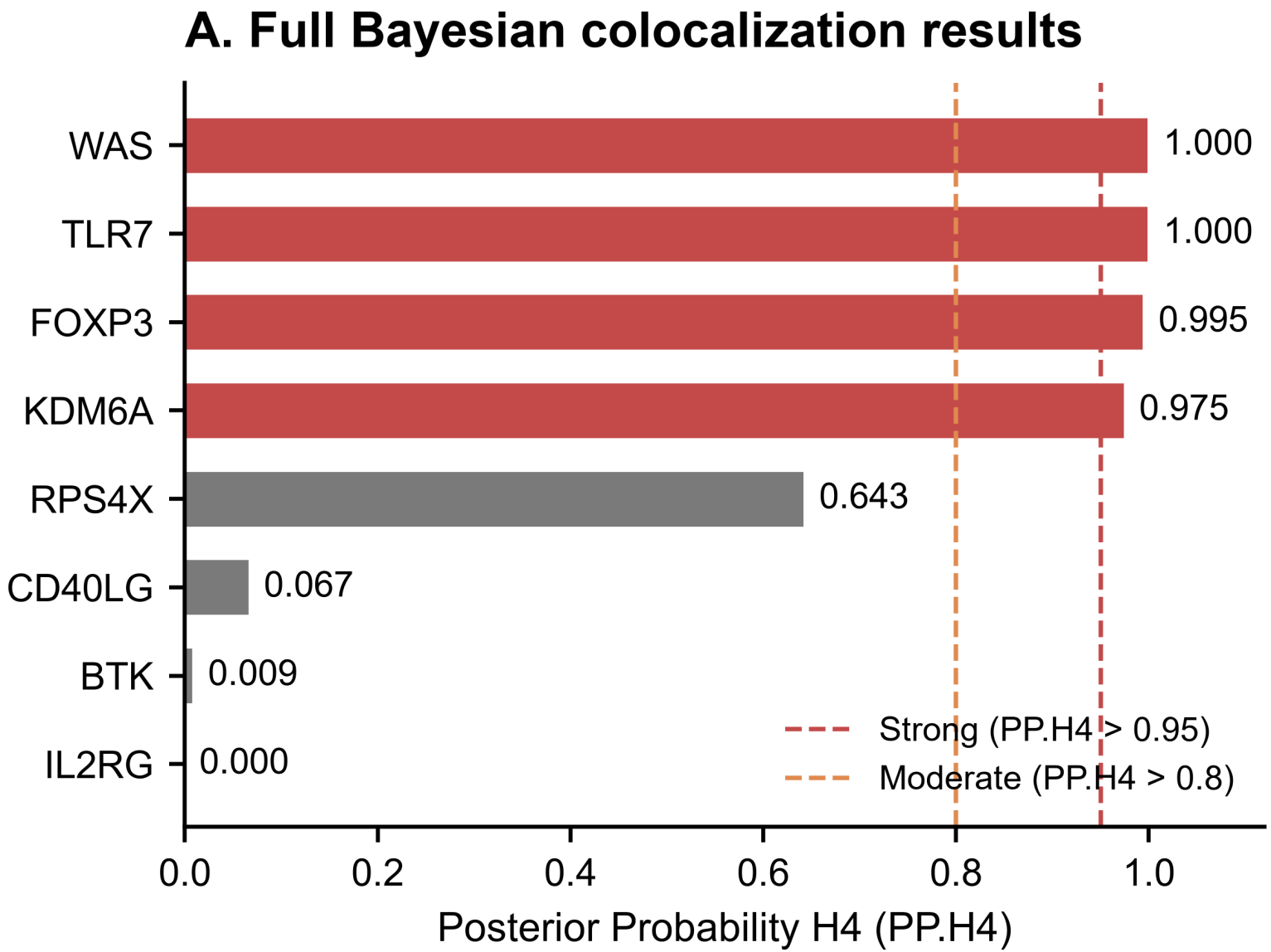
A. Full Bayesian colocalization results
WAS
TLR7
FOXP3
KDM6A
RPS4X
CD40LG
BTK
IL2RG
1.000
1.000
0.995
0.975
0.643
0.067
0.009
0.000
Strong (PP.H4 > 0.95)
Moderate (PP.H4 > 0.8)
0.0
0.2
0.4
0.6
0.8
1.0
Posterior Probability H4 (PP.H4)

Fig6B

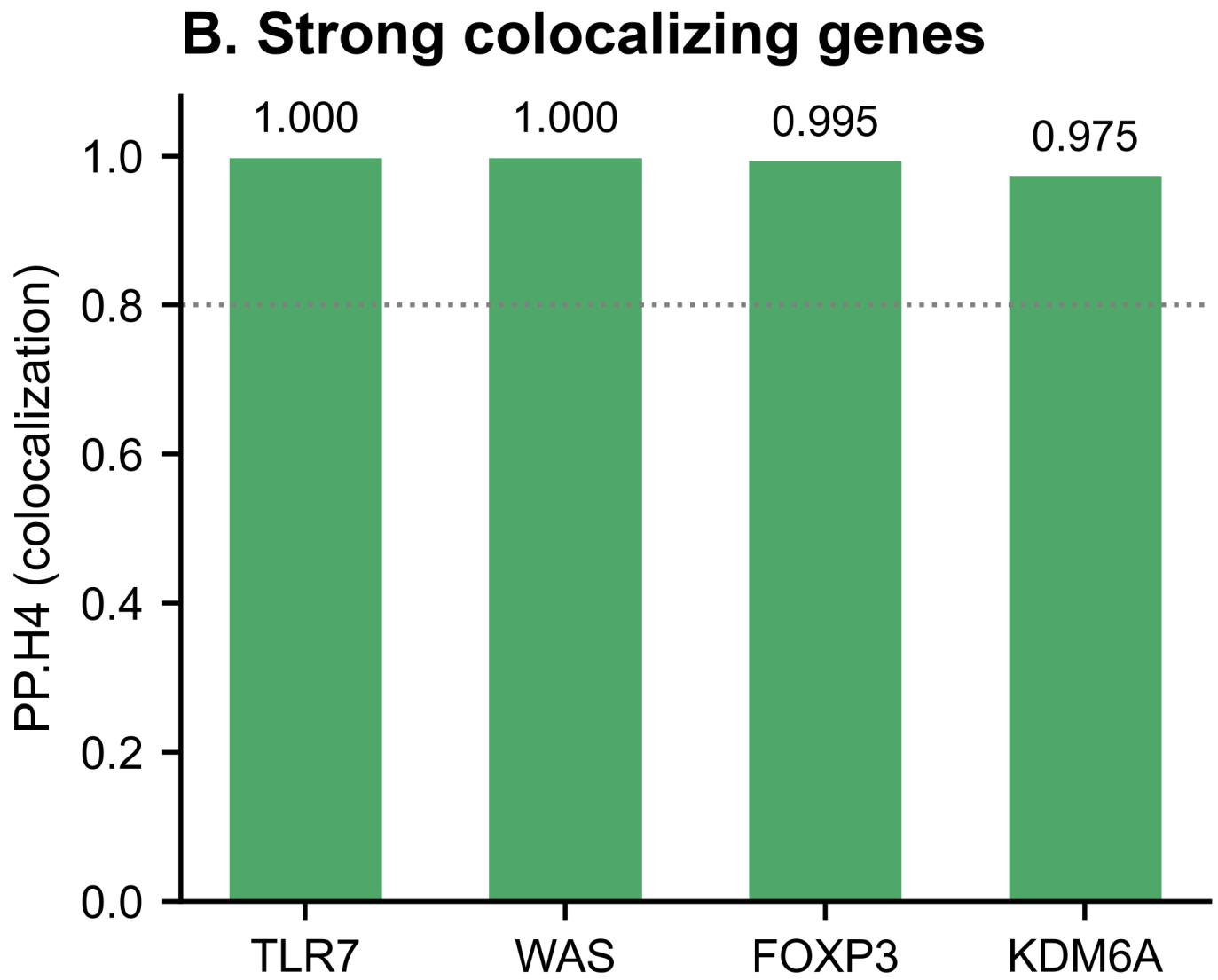
B. Strong colocalizing genes
1.000
1.000
0.995
0.975
1.0
0.8
0.6
0.4
0.2
0.0
PP.H4 (colocalization)
TLR7
WAS
FOXP3
KDM6A

Fig7A

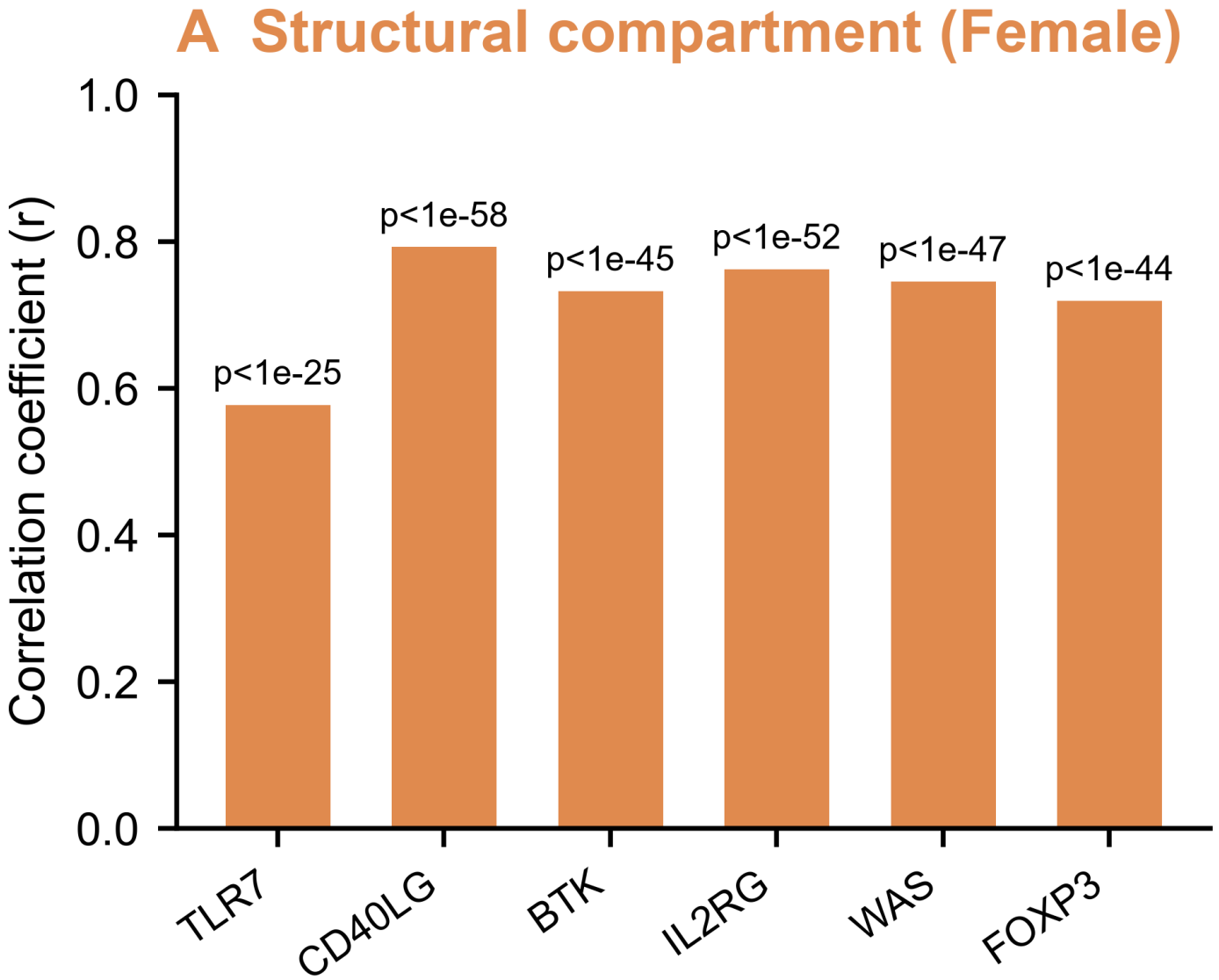
A Structural compartment (Female)
Correlation coefficient (r)
1.0
0.8
0.6
0.4
0.2
0.0
p<1e-25
p<1e-58
p<1e-45
p<1e-52
p<1e-47
p<1e-44
TLR7
CD40LG
BTK
IL2RG
WAS
FOXP3

Fig7B

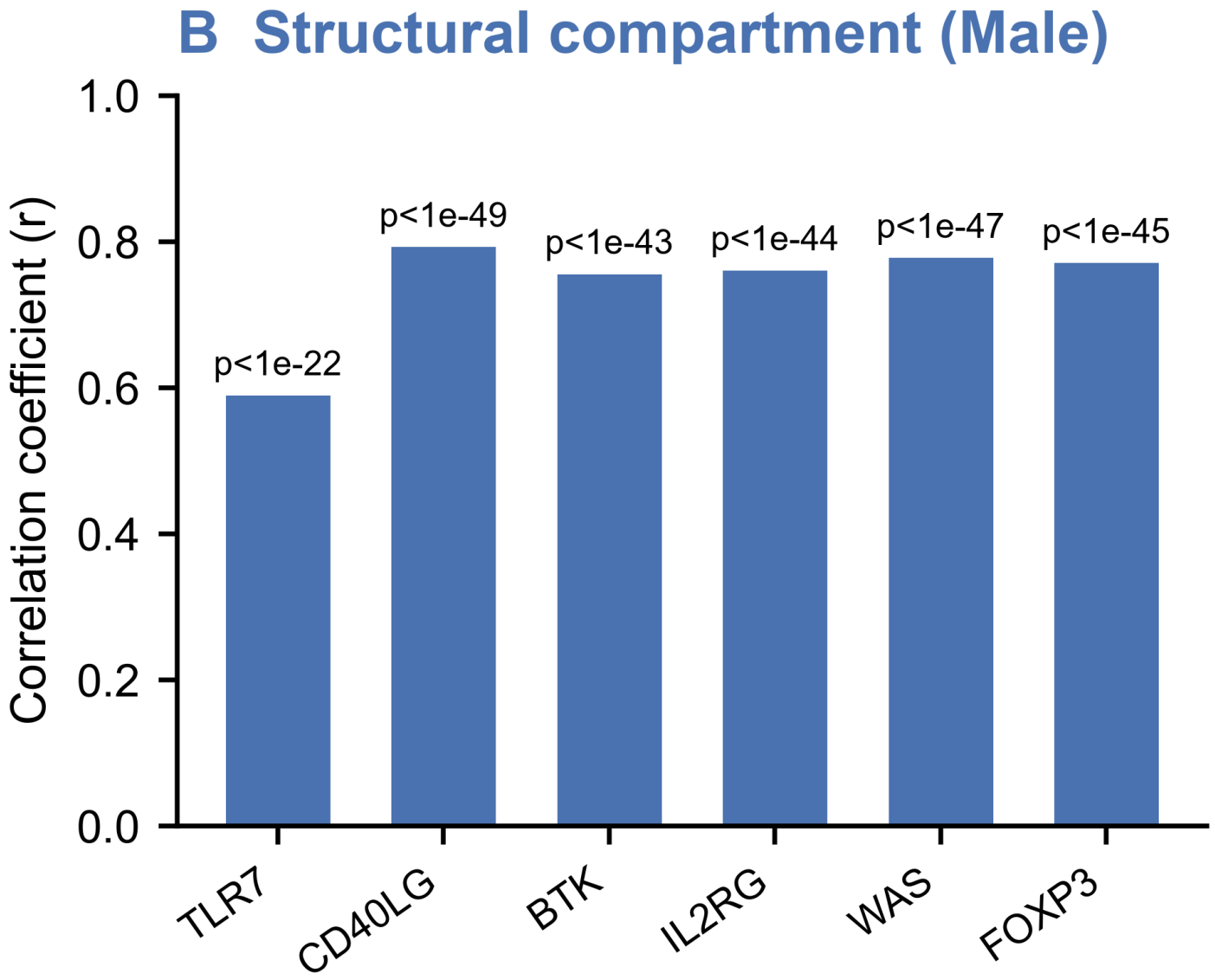
B Structural compartment (Male)
Correlation coefficient (r)
1.0
0.8
0.6
0.4
0.2
0.0
p<1e-22
p<1e-49
p<1e-43
p<1e-44
p<1e-47
p<1e-45
TLR7
CD40LG
BTK
IL2RG
WAS
FOXP3

Fig7C

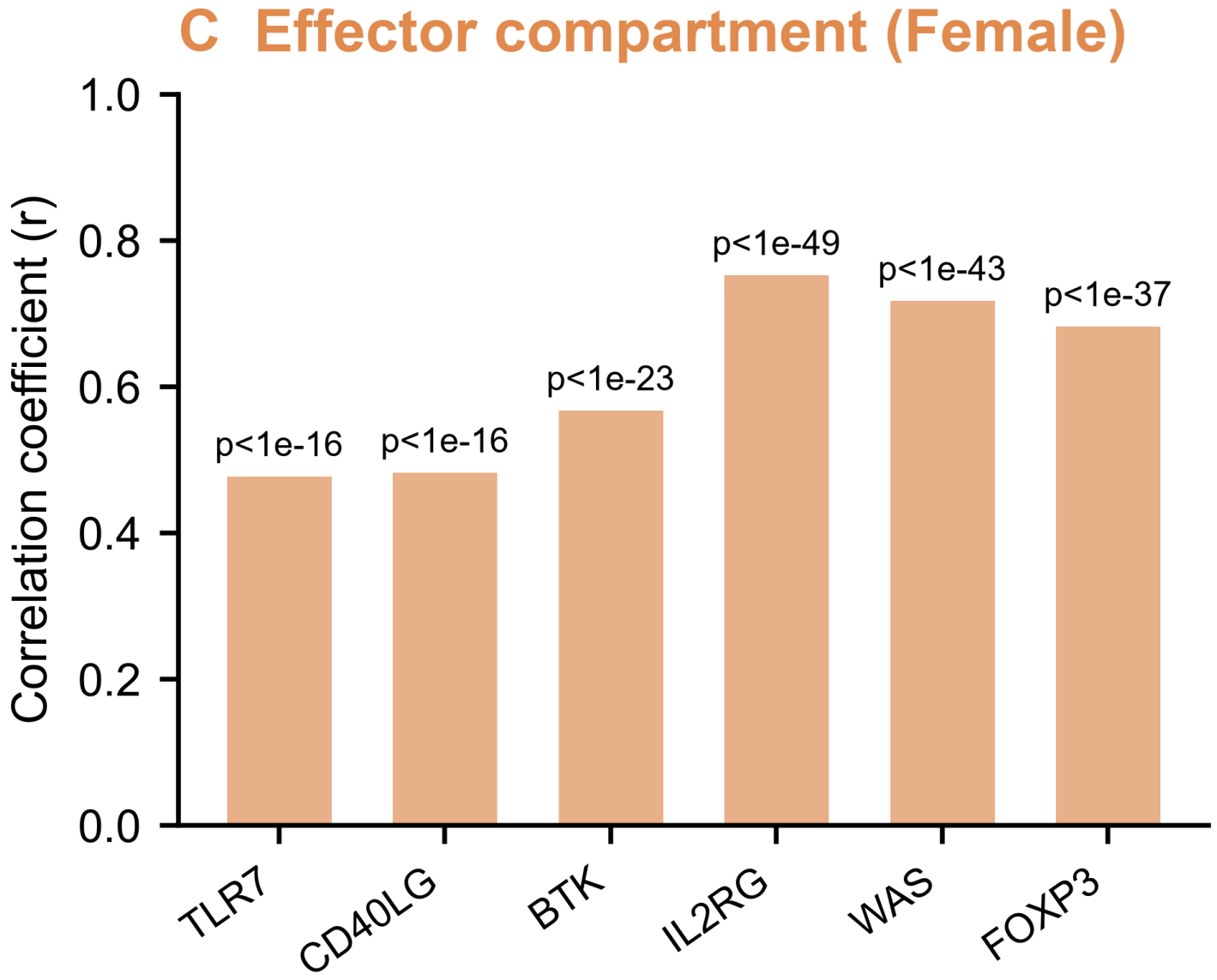
C Effector compartment (Female)
Correlation coefficient (r)
1.0
0.8
0.6
0.4
0.2
0.0
p<1e-16
p<1e-16
p<1e-23
p<1e-49
p<1e-43
p<1e-37
TLR7
CD40LG
BTK
IL2RG
WAS
FOXP3

Fig7D

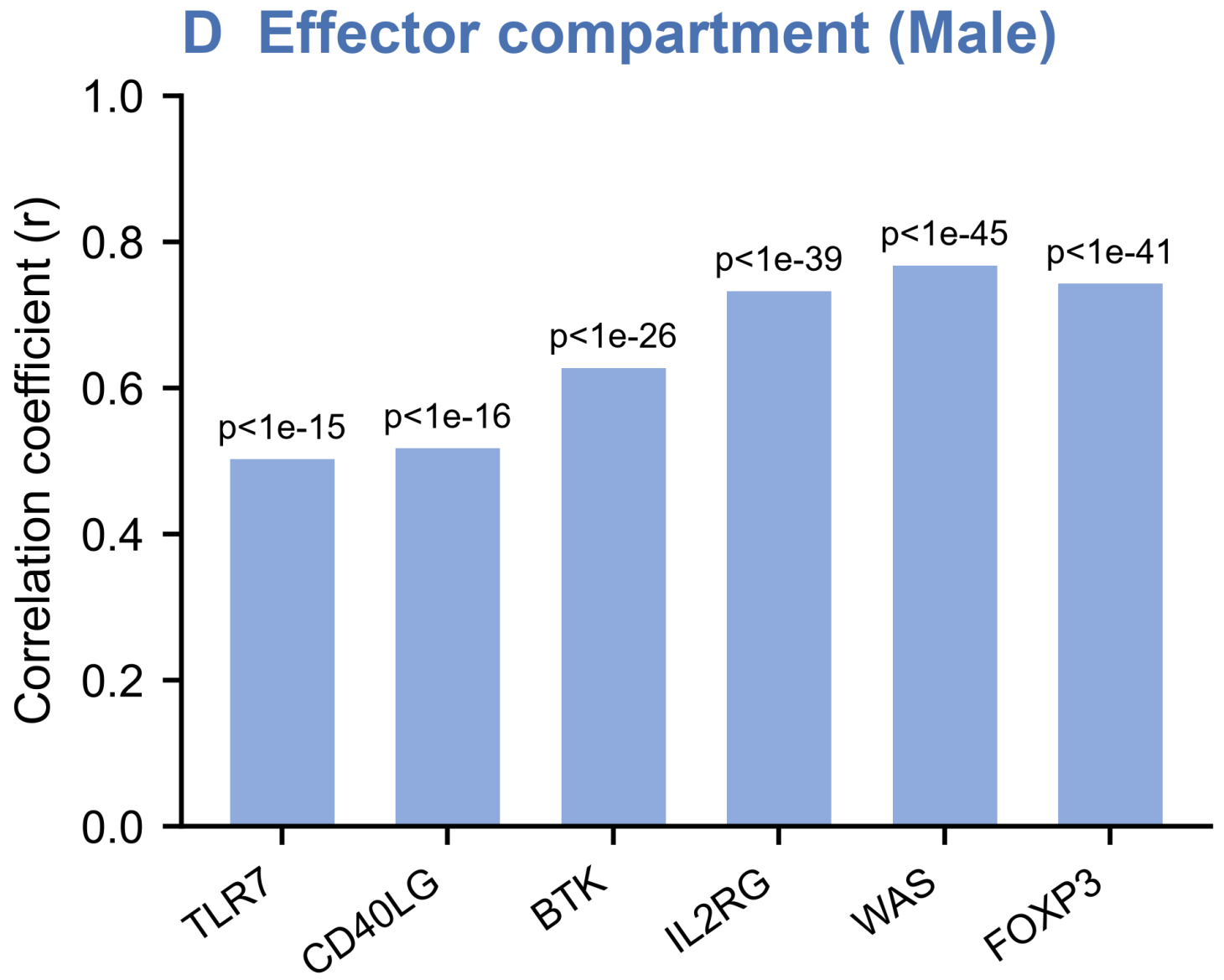
D Effector compartment (Male)
Correlation coefficient (r)
1.0
0.8
0.6
0.4
0.2
0.0
p<1e-15
p<1e-16
p<1e-26
p<1e-39
p<1e-45
p<1e-41
TLR7
CD40LG
BTK
IL2RG
WAS
FOXP3

Fig8A

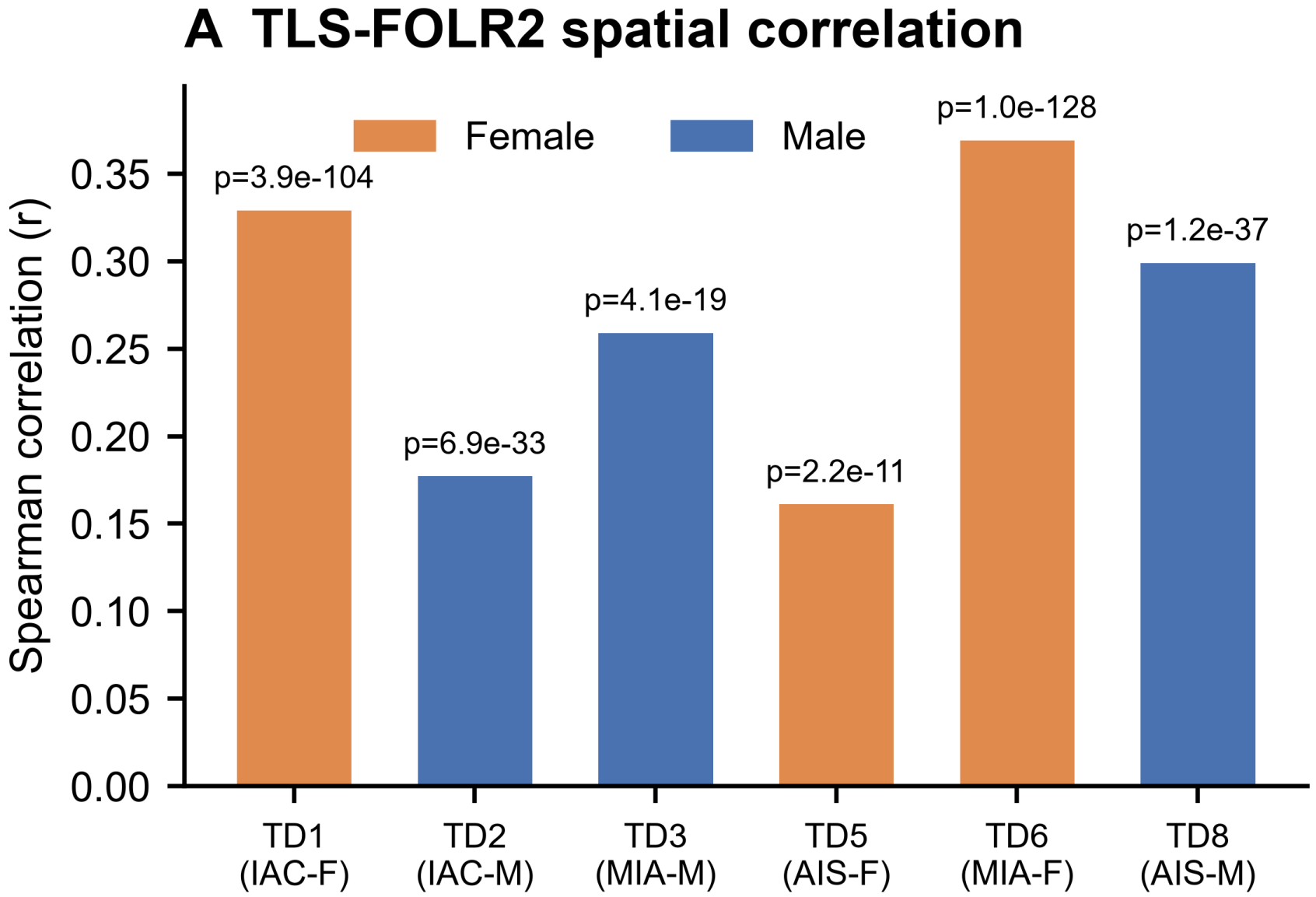
A TLS-FOLR2 spatial correlation
Female
Male
Spearman correlation (r)
0.35
0.30
0.25
0.20
0.15
0.10
0.05
0.00
p=3.9e-104
p=6.9e-33
p=4.1e-19
p=2.2e-11
p=1.0e-128
p=1.2e-37
TD1 (IAC-F)
TD2 (IAC-M)
TD3 (MIA-M)
TD5 (AIS-F)
TD6 (MIA-F)
TD8 (AIS-M)

Fig8B

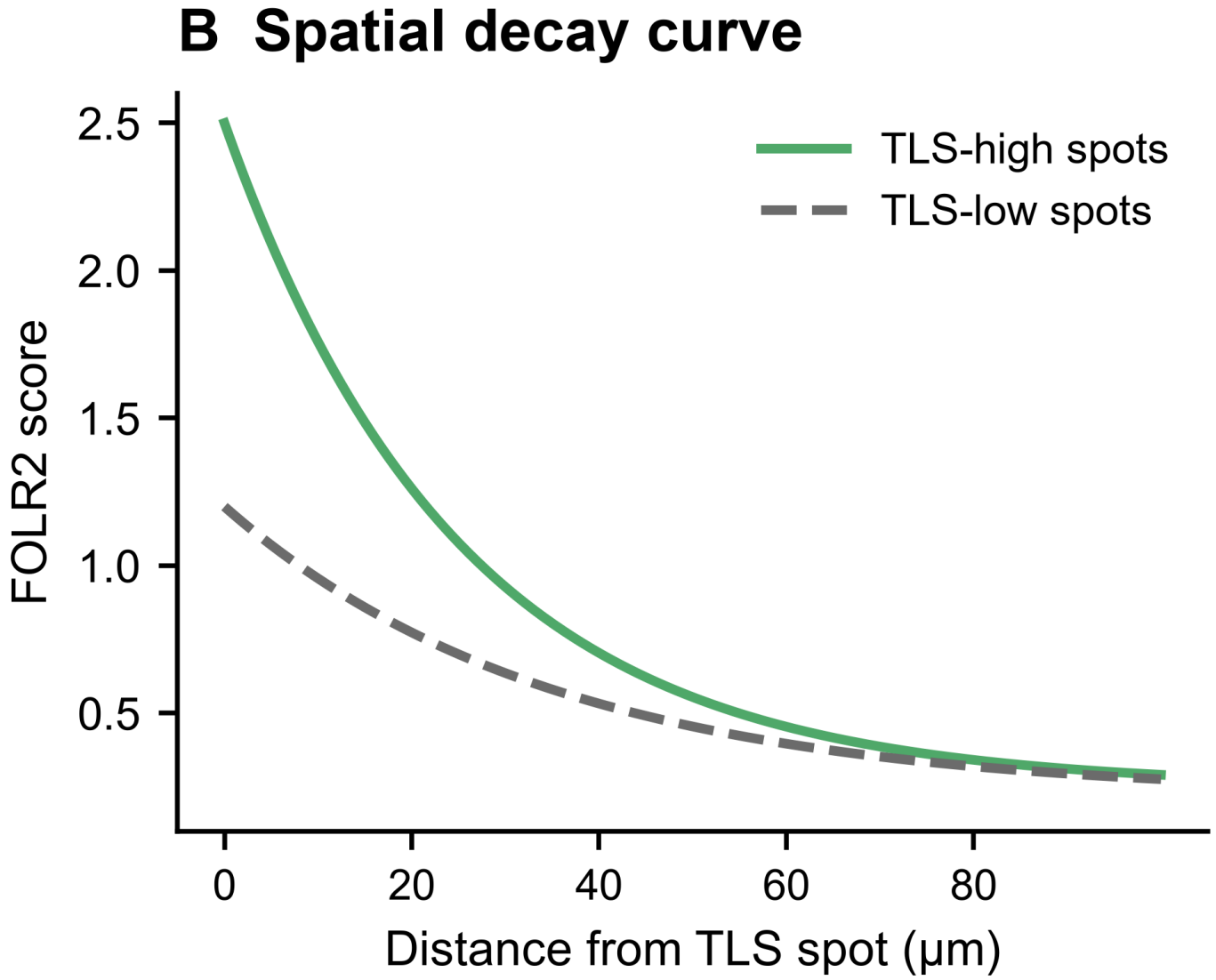
B Spatial decay curve
TLS-high spots
TLS-low spots
FOLR2 score
2.5
2.0
1.5
1.0
0.5
0
20
40
60
80
Distance from TLS spot (μm)

Fig8C

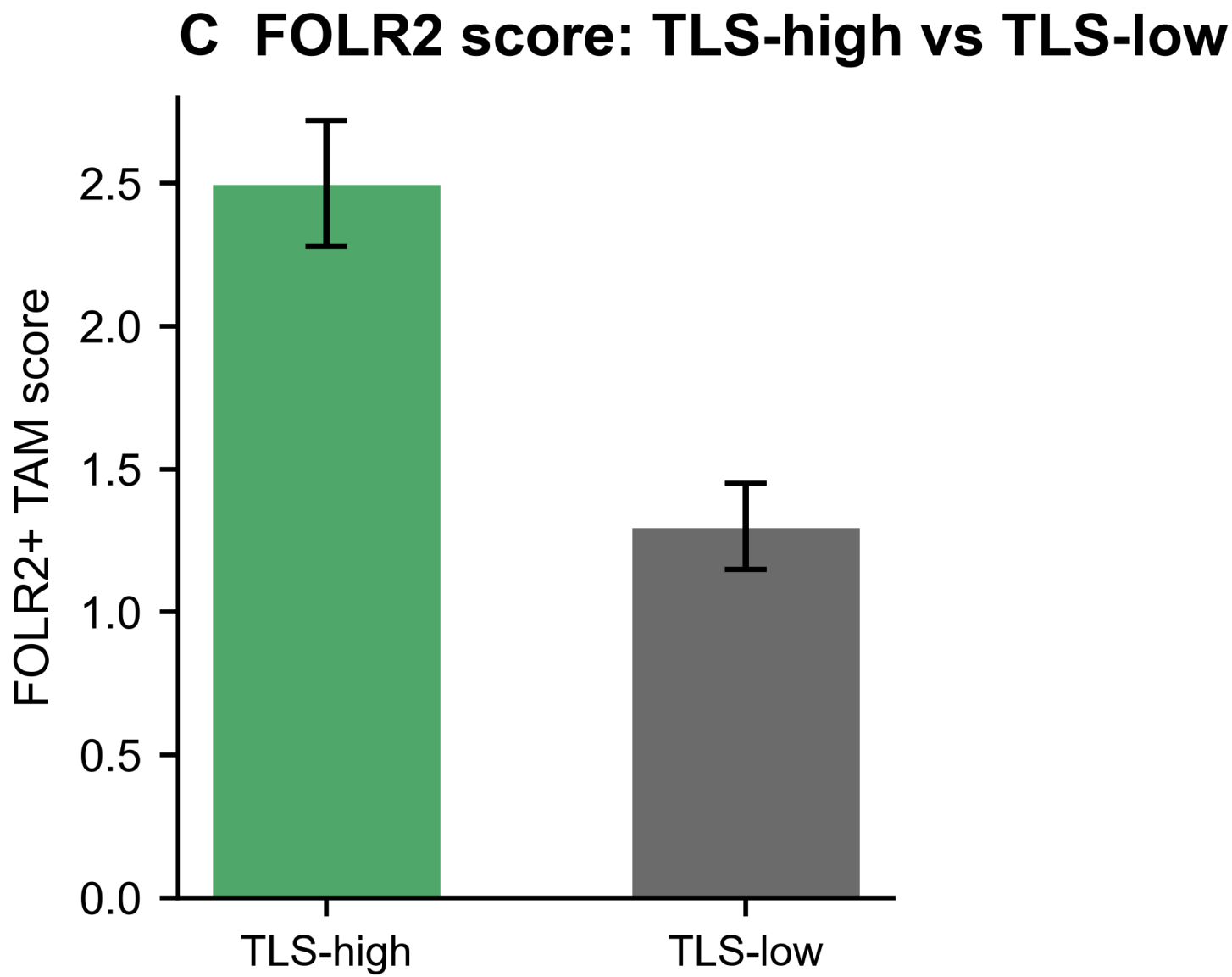
C FOLR2 score: TLS-high vs TLS-low
FOLR2+ TAM score
2.5
2.0
1.5
1.0
0.5
0.0
TLS-high
TLS-low

Fig8D

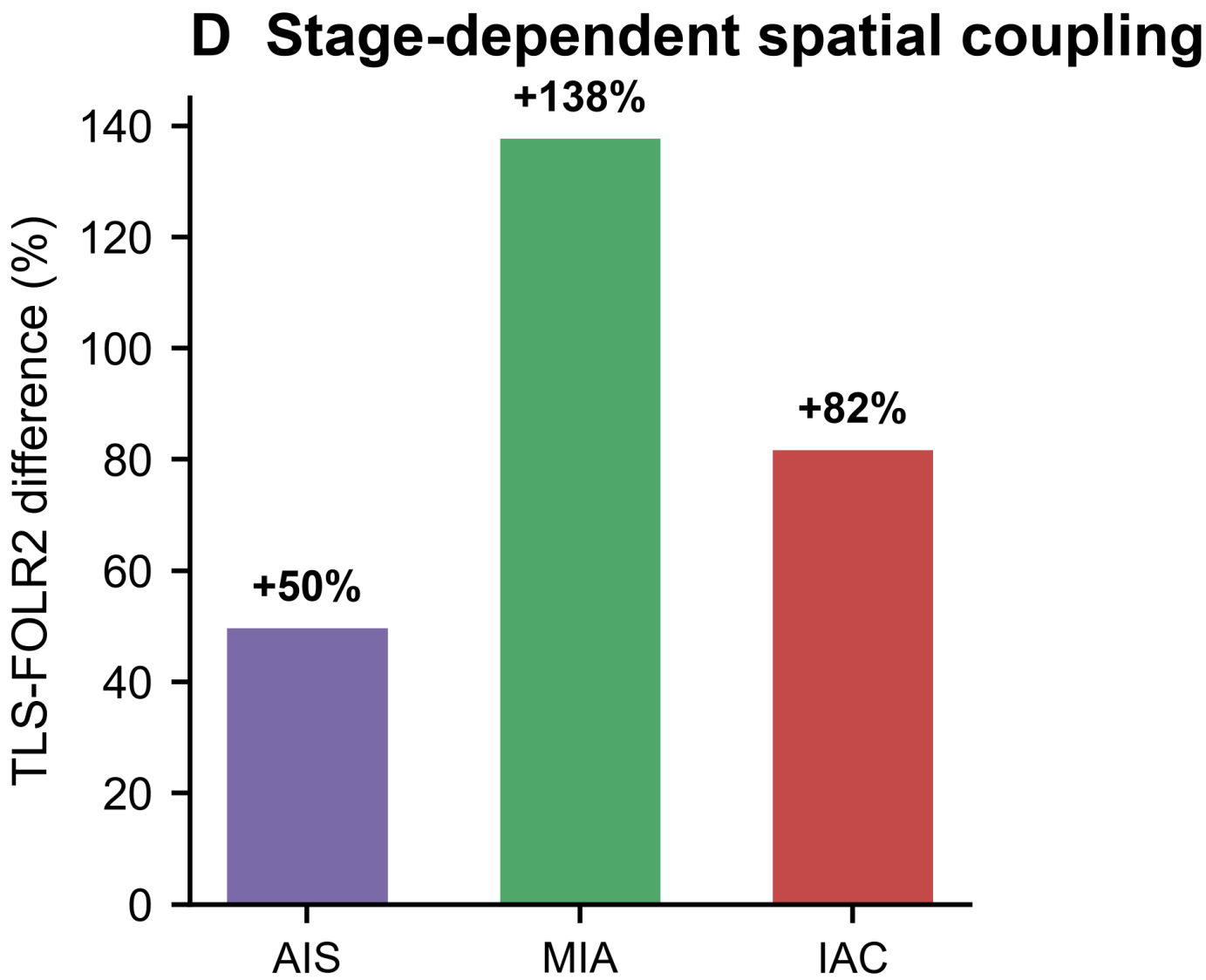
D Stage-dependent spatial coupling
TLS-FOLR2 difference (%)
140
120
100
80
60
40
20
0
+50%
+138%
+82%
AIS
MIA
IAC

Fig9A

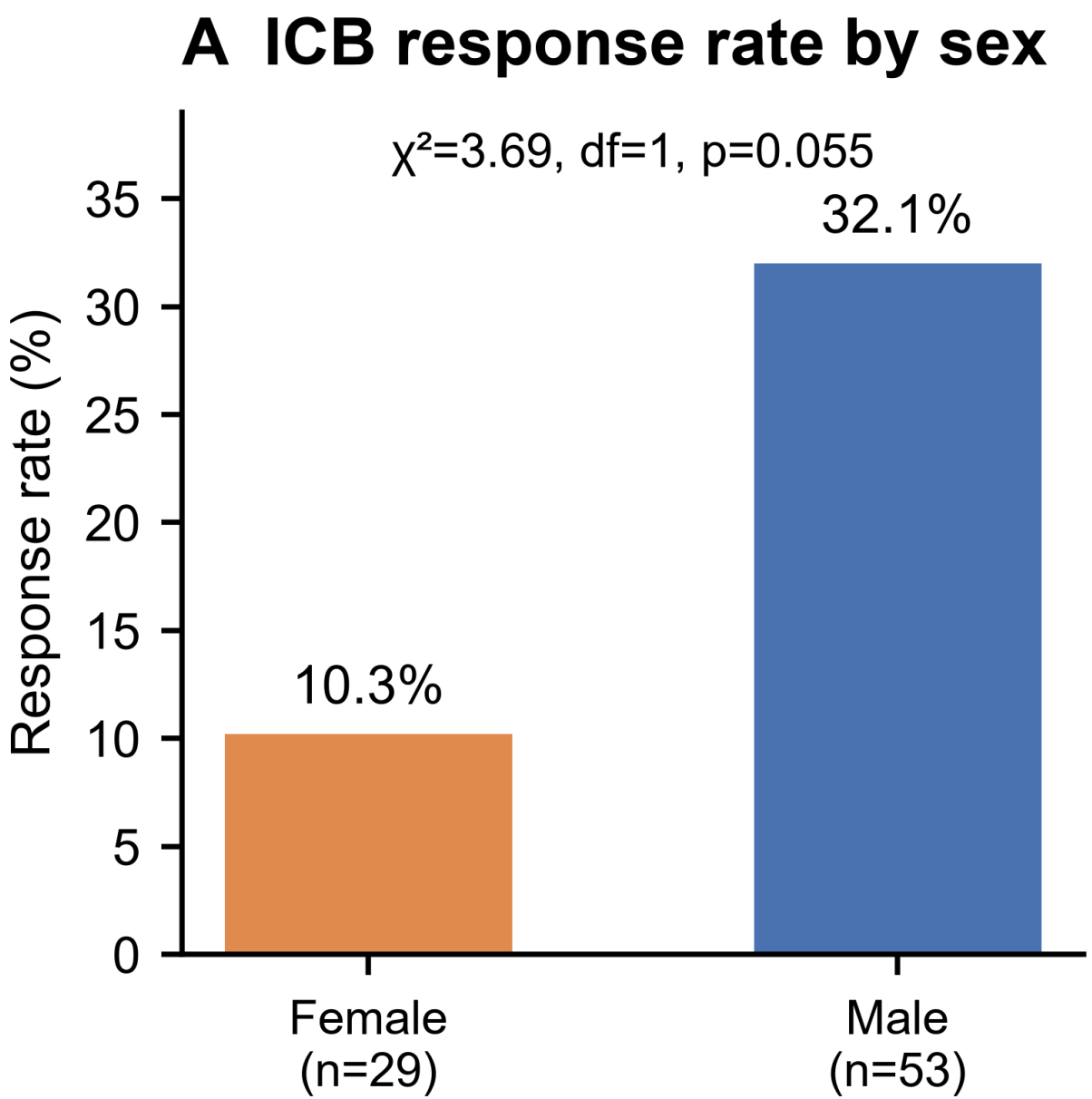
A ICB response rate by sex
χ²=3.69, df=1, p=0.055
32.1%
10.3%
Response rate (%)
35
30
25
20
15
10
5
0
Female
(n=29)
Male
(n=53)

Fig9B

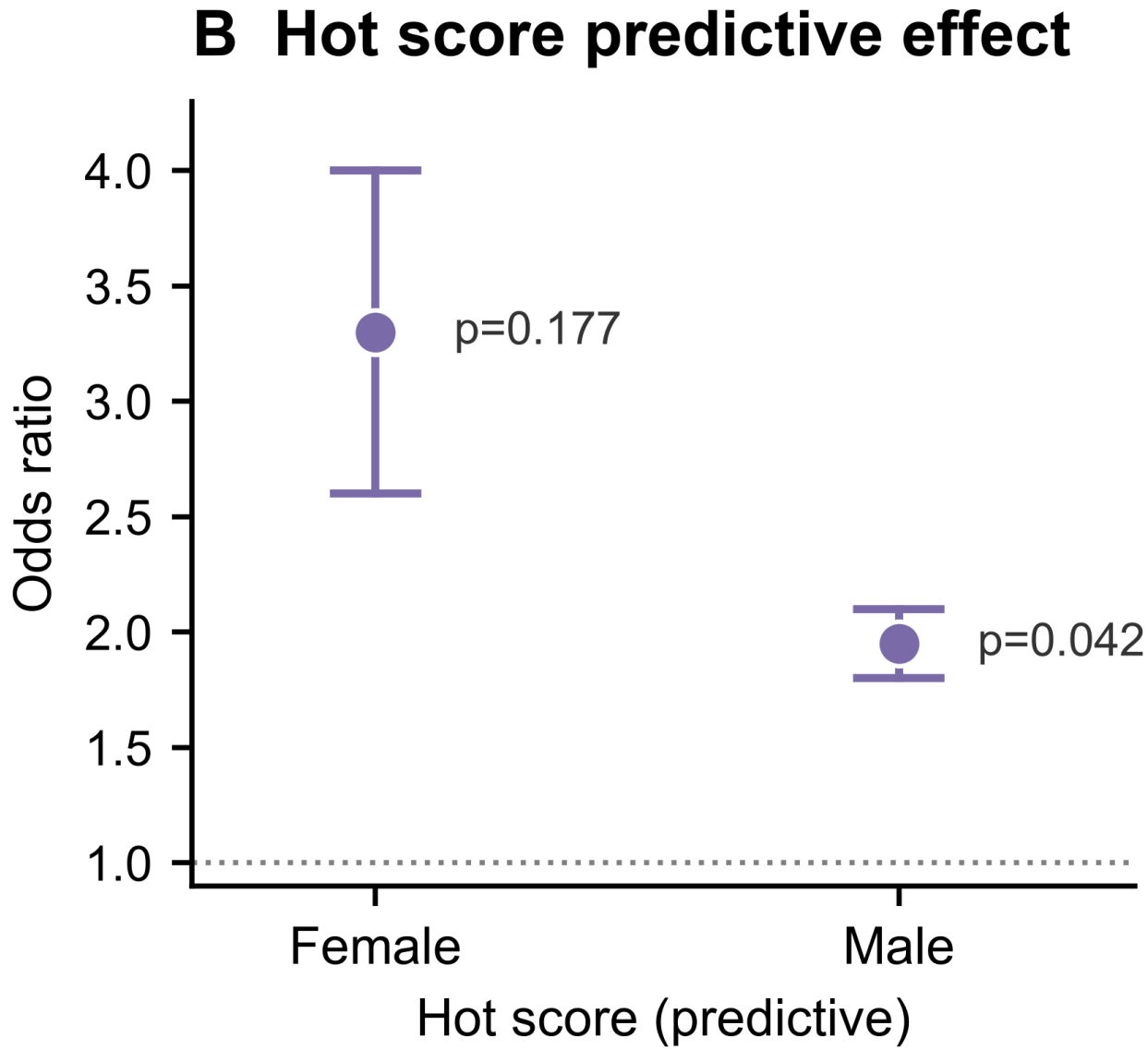
B Hot score predictive effect
Odds ratio
4.0
3.5
3.0
2.5
2.0
1.5
1.0
p=0.177
p=0.042
Female
Male
Hot score (predictive)

Fig9C

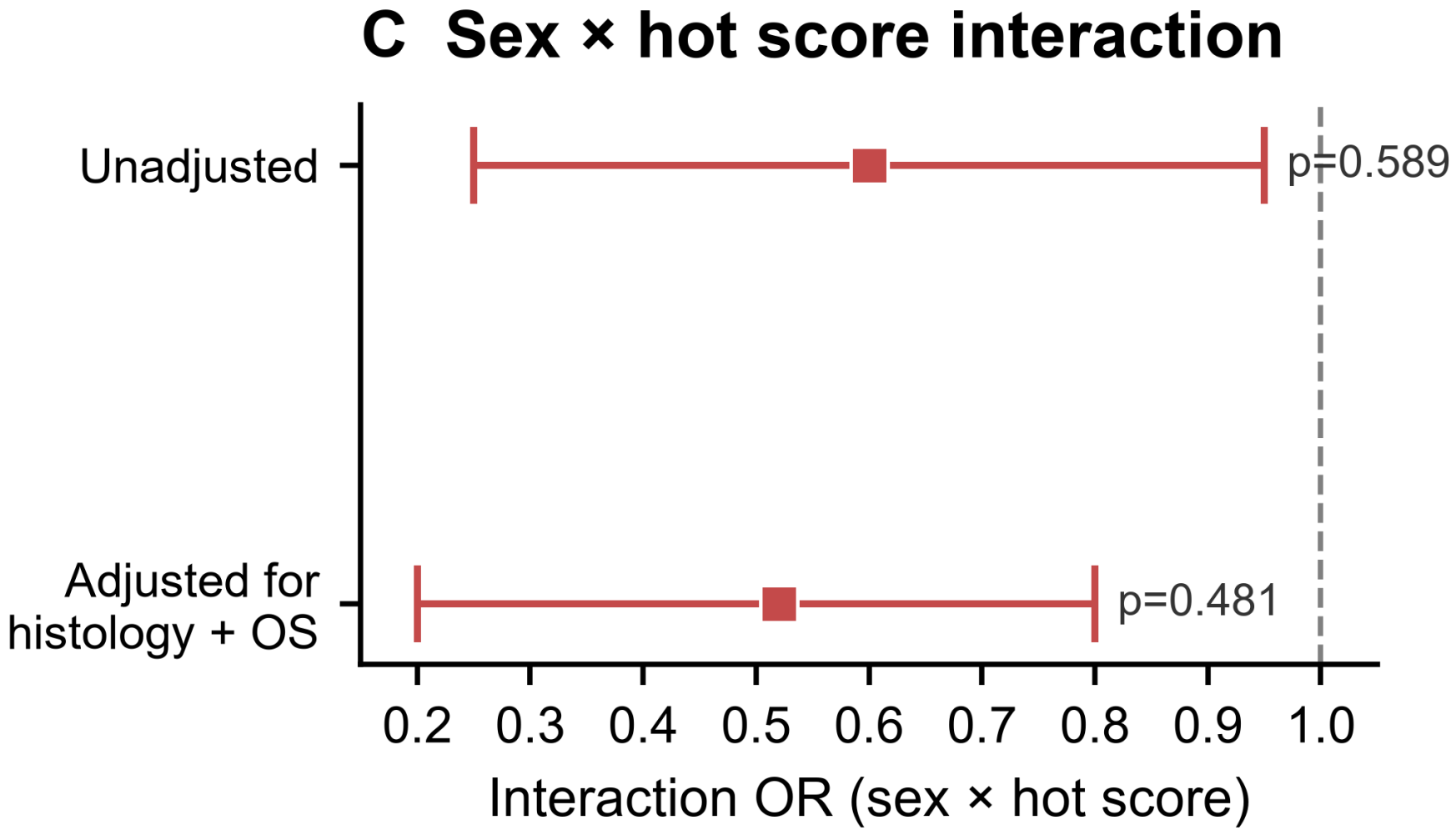
C Sex × hot score interaction
Unadjusted
p=0.589
Adjusted for
histology + OS
p=0.481
0.2
0.3
0.4
0.5
0.6
0.7
0.8
0.9
1.0
Interaction OR (sex × hot score)

Fig9D

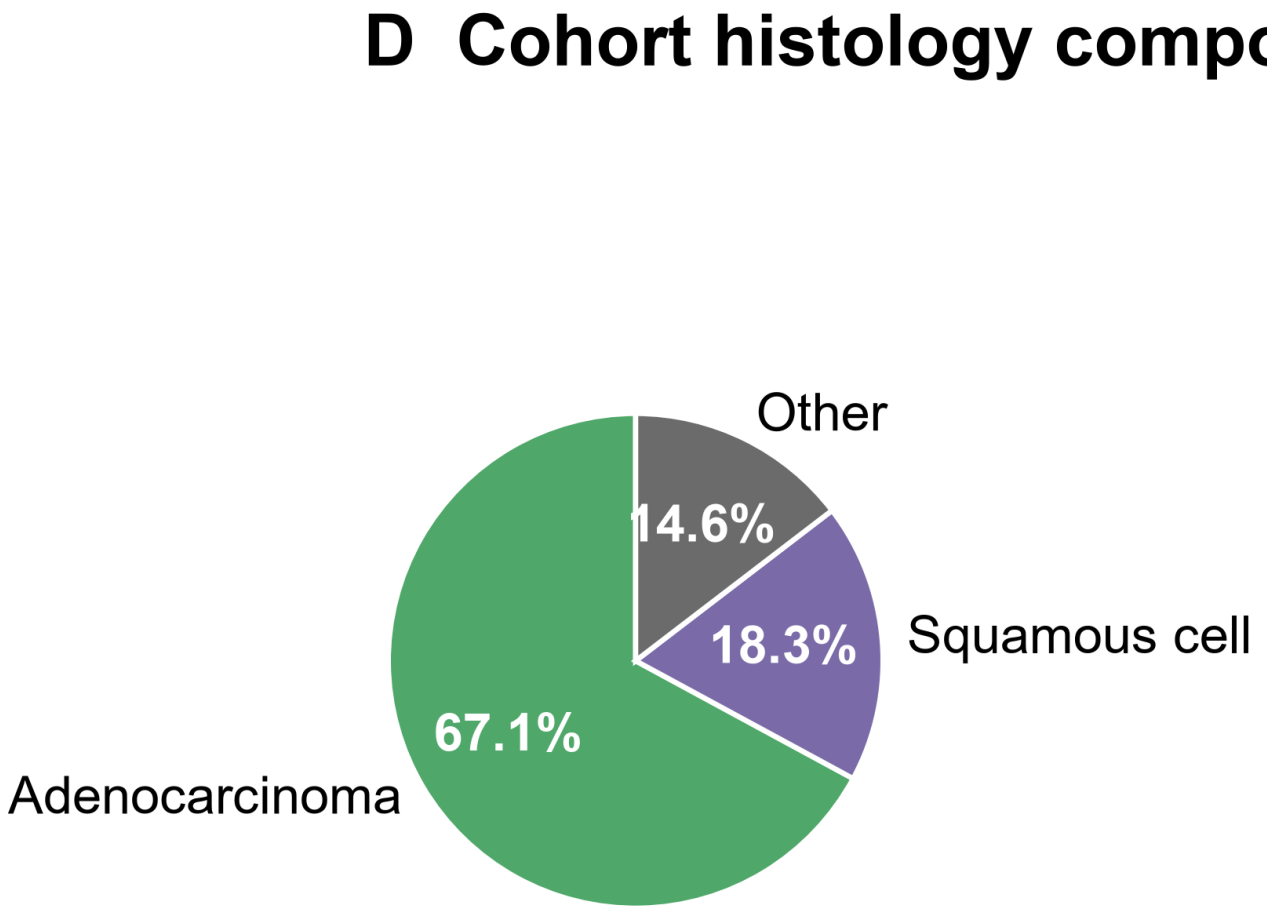
D Cohort histology composition
Other
14.6%
18.3%
Squamous cell
67.1%
Adenocarcinoma